Karlsruhe Institute of Technology

wave phenomena
analysis and numerics

A post-processed higher-order multiscale method for nondivergence-form elliptic equations

Moritz Hauck, Roland Maier, Timo Sprekeler

CRC Preprint 2026/13, April 2026

KARLSRUHE INSTITUTE OF TECHNOLOGY

CRC 1173

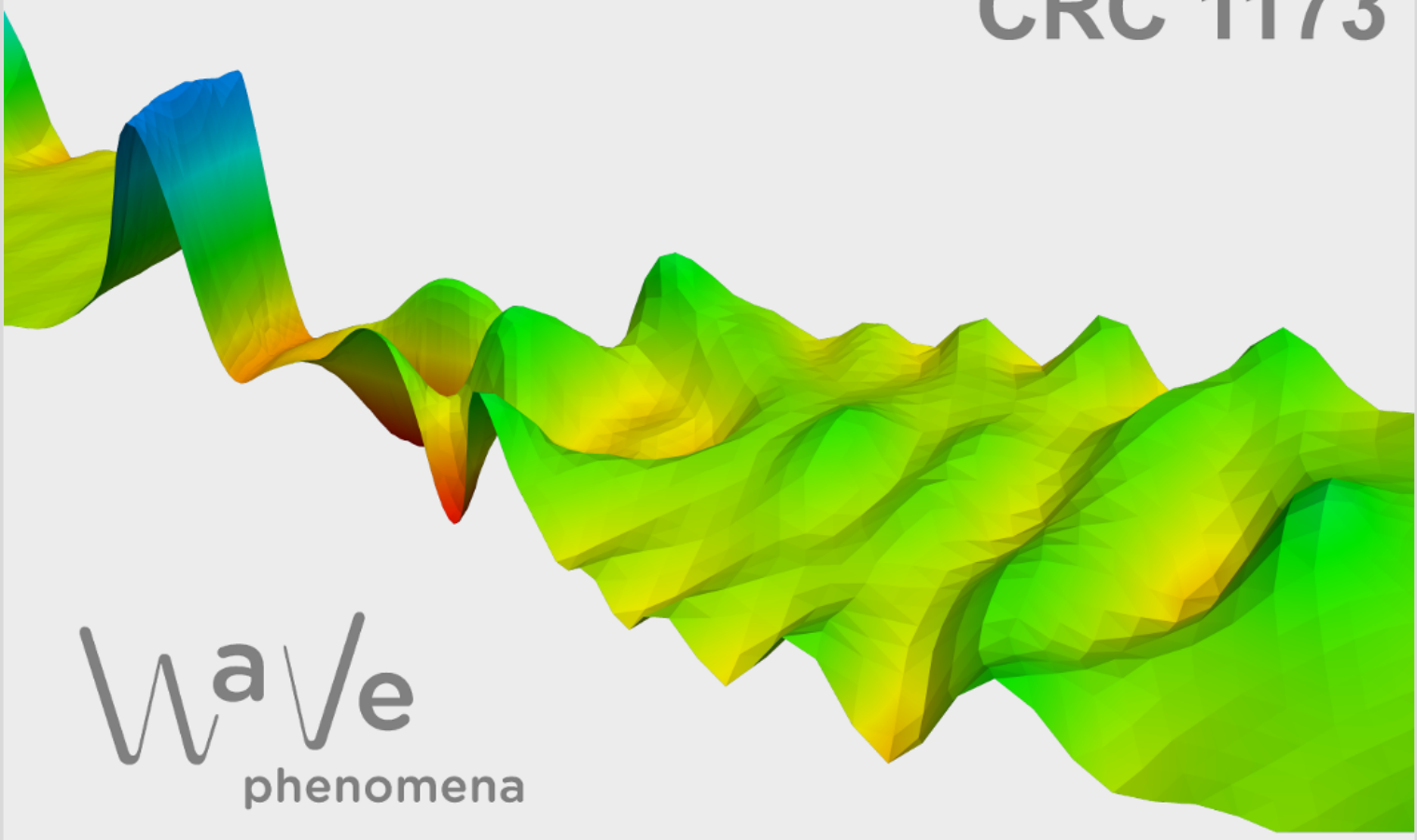

Participating universities

Funded by

ISSN 2365-662X

A POST-PROCESSED HIGHER-ORDER MULTISCALE METHOD FOR NONDIVERGENCE-FORM ELLIPTIC EQUATIONS

MORITZ HAUCK*, ROLAND MAIER*, TIMO SPREKELER†

Abstract. We study the finite element approximation of linear second-order elliptic partial differential equations in nondivergence form with highly heterogeneous diffusion and drift coefficients. A generalized Cordes condition is imposed to guarantee that a suitably renormalized version of the nondivergence-form differential operator is near the Laplacian. Based on a stabilized symmetric formulation for the gradient that enables the use of H^1-conforming approximation spaces, we construct a multiscale method following the methodology of the localized orthogonal decomposition with coarse basis functions tailored to the heterogeneous coefficients. We employ a novel post-processing strategy to obtain higher-order convergence rates, overcoming previous limitations imposed by the low regularity of the load functional. Numerical experiments demonstrate the performance of the method.

1. Introduction

On a bounded convex polyhedral domain $\Omega \subset \mathbb{R}^d$ in dimension $d \in \{2,3\}$, we consider the numerical approximation of the homogeneous Dirichlet problem

$$\begin{cases} Lu = f & \text{in } \Omega, \\ u = 0 & \text{on } \partial\Omega, \end{cases} \tag{1.1}$$

where $f \in L^2(\Omega)$ is a given source term and L is a linear second-order differential operator in nondivergence form defined by

$$Lv \coloneqq A : D^2 v + b \cdot \nabla v = \sum_{i,j=1}^{d} a_{ij}\, \partial_{ij}^2 v + \sum_{k=1}^{d} b_k\, \partial_k v,$$

involving a uniformly elliptic diffusion coefficient $A = (a_{ij})_{1\le i,j\le d} \in L^\infty(\Omega; \mathbb{R}^{d\times d}_{\mathrm{sym}})$ and a drift coefficient $b = (b_k)_{1\le k\le d} \in L^\infty(\Omega;\mathbb{R}^d)$. Our focus is on regimes where the coefficients are multiscale, exhibiting strong oscillations across multiple, nonseparated scales. Motivated by the fact that, in the absence of any further structural assumptions, the map $L\colon H^2(\Omega)\cap H^1_0(\Omega) \to L^2(\Omega)$ is not bijective in general, we impose the following Cordes-type condition:

$$\exists\, \delta \in \left(\frac{\eta}{1+C_{\mathrm{P}}^2}\,, 1 \right] : \quad \frac{A : A + b\cdot b}{(\mathrm{tr}(A))^2} \le \frac{1}{d-1+\delta} \quad \text{a.e. in } \Omega, \tag{1.2}$$

where the constant $C_{\mathrm{P}} \coloneqq \inf_{\varphi\in V\setminus\{0\}} \|D\varphi\|_{L^2(\Omega)}/\|\varphi\|_{L^2(\Omega)} > 0$ is the optimal Poincaré constant for the subspace $V \coloneqq H^1_t(\Omega;\mathbb{R}^d)$ of $H^1(\Omega;\mathbb{R}^d)$ consisting of functions with vanishing tangential trace on $\partial\Omega$, and the constant $\eta \in \{0,1\}$ is given by $\eta \coloneqq 0$ if $b = 0$ almost everywhere in Ω, and $\eta \coloneqq 1$ otherwise.

2020 *Mathematics Subject Classification.* 65N12, 65N15, 65N30.

Key words and phrases. nondivergence-form PDE, Cordes condition, a priori error analysis, multiscale methods, localized orthogonal decomposition.

Condition (1.2) generalizes the classical Cordes condition for operators of the form $v \mapsto A : D^2 v$ (see [Cor56]), and is inspired by the Cordes-type condition

$$\exists\, (\epsilon, l) \in (0,1] \times (0,\infty) : \qquad \frac{A : A + \frac{1}{2l}(b \cdot b) + \frac{1}{l^2} c^2}{(\operatorname{tr}(A) + \frac{1}{l} c)^2} \leq \frac{1}{d + \epsilon} \quad \text{a.e. in } \Omega \tag{1.3}$$

for operators of the form $v \mapsto A : D^2 v + b \cdot \nabla v - cv$ (see [SS14]). The need for a new condition comes from the observation that (1.3) cannot be satisfied when $c = 0$ almost everywhere in Ω. In terms of Campanato's notion of near operators [Cam94], the Cordes-type condition (1.2) ensures that a suitably renormalized version of L is near the Laplacian, which in turn implies existence and uniqueness of a strong solution $u \in H^2(\Omega) \cap H^1_0(\Omega)$ to problem (1.1).

The goal of this work is the construction and rigorous error analysis of a method for the accurate numerical approximation of the multiscale problem (1.1), a task often referred to as numerical homogenization. We follow the methodology of localized orthogonal decomposition (LOD) [MP14, MP20, AHP21], using the observation that $z = \nabla u$ is the unique element in V such that

$$\forall \varphi \in V : \qquad (\tilde{L} z, \tilde{L} \varphi)_{L^2(\Omega)} + \sigma(\operatorname{rot}(z), \operatorname{rot}(\varphi))_{L^2(\Omega)} = (f, \tilde{L}\varphi)_{L^2(\Omega)} \tag{1.4}$$

with $\tilde{L}\varphi \coloneqq A : D\varphi + b \cdot \varphi$ for $\varphi \in V$, and $\sigma > 0$ a chosen constant. Inspired by [Gal17, Gal19], this formulation has the important advantage that it is symmetric and allows for a discretization based on classical H^1-conforming finite element spaces. In particular, we can avoid the more technical implementation of H^2-conforming discretizations; see, e.g., [KM19]. Once a practical multiscale approximation of z has been obtained, the function u can be easily recovered by a computationally cheap finite element approximation of a Poisson problem on a coarse mesh.

For recent developments in homogenization of nondivergence-form equations, we refer the reader to [GTY20, ST21, Spr24, GST25a] for periodic homogenization and [AFL22, GT24, GT25, GST25b] for stochastic homogenization. Various numerical schemes for the approximation of effective diffusion matrices in periodic homogenization of nondivergence-form equations have been proposed in recent years; see [CSS20, SSZ25] for finite element methods, [FO09] for a finite difference method, and [SWZ25] for a Lagrangian method. Linear elliptic equations in nondivergence-form arise as linearizations of fully nonlinear second-order Hamilton–Jacobi–Bellman and Isaacs equations. Numerical schemes for the approximation of effective Hamiltonians arising in the periodic homogenization of such problems have recently been developed; see [GSS21, KS22, QSTY24] for finite element methods and [CM09, FO18a, FO18b] for finite difference methods.

The sole reference for the numerical homogenization of nondivergence-form equations with arbitrarily rough coefficients beyond periodicity and scale separation is the H^2-conforming LOD method proposed in [FGPS24], which is based on a nonsymmetric formulation and provides an error bound in the H^1-norm only. In contrast, the method developed in this work does not require H^2-conforming elements, is based on a symmetric formulation, allows for higher-order approximation, and admits provable error bounds for the approximation of second-order derivatives of u in the L^2-norm. We employ the localization strategy proposed in [HLM26], eliminating the undesirable numerical effects observed in [FGPS24] that degrade approximation quality for fixed localization parameters. Further, we employ a post-processing step, which enables the extraction of high-order convergence rates in the spirit of higher-order LOD approaches; see [Mai21, DHM23]. We incorporate ideas from the collocation version of the Super-LOD method introduced in [HP22b] as well as strategies for additional corrections as analyzed in [HM19, KKMW25].

Similar constructions for the functionals that implicitly define the LOD approximation space, often called quantities of interest, have also been investigated in [HHM16, HL25a, HL25b, HLS26] for mixed formulations of divergence-form problems.

This paper is structured as follows. In Section 2, we show the existence and uniqueness of a strong solution u to (1.1) under the Cordes-type condition (1.2), analyze the variational problem (1.4) for ∇u, and discuss the recovery of u. In Section 3, we introduce and rigorously analyze an ideal numerical homogenization method that achieves optimal-order approximations without pre-asymptotic effects. In Section 4, we prove exponential decay properties for a problem-adapted orthogonal projection $\mathcal{R}$ onto the ideal multiscale space, as well as of related operators. These results are then used in Section 5 to localize the operator $\mathcal{R}$. In Section 6, we introduce and rigorously analyze a practical numerical homogenization method based on locally computed basis functions, justified by the exponential decay properties and localization obtained in the previous sections. Finally, in Section 7, we provide various numerical experiments that illustrate the theoretical results.

Notation. Throughout this work, we use the notation $a \lesssim b$ (respectively $a \gtrsim b$) to indicate that $a \leq C\, b$ (respectively $a \geq C\, b$), where $C > 0$ denotes a generic constant independent of the coarse mesh size H, the localization parameter ℓ, and the oscillatory behavior of the solution u. The constant C may depend on the mesh regularity, the spatial dimension d, the ellipticity constants ν_1, ν_2, the $L^\infty(\Omega)$-bound of b, the Cordes parameter δ, the stabilization parameter σ, and the post-processing order p. We employ standard notation for Lebesgue and Sobolev spaces and their associated norms. For norms defined on the entire domain Ω, such as the $L^p(\Omega)$-norm, we write $\|\cdot\|_{L^p}$, omitting the domain from the notation. The domain is specified explicitly only when referring to proper subdomains of Ω. The gradient and the Hessian of a scalar-valued function u are denoted by ∇u and $D^2 u$, respectively. The Jacobian of a vector-valued function v is denoted by Dv. Finally, we write $x \cdot y \coloneqq x^{\mathrm{T}} y$ for $x, y \in \mathbb{R}^d$, and $X : Y \coloneqq \operatorname{tr}(X^{\mathrm{T}} Y)$ for $X, Y \in \mathbb{R}^{d\times d}$.

2. Model problem

Let $\Omega \subset \mathbb{R}^d$ be a bounded convex domain in dimension $d \in \{2, 3\}$. We consider the elliptic nondivergence-form problem

$$\begin{cases} A : D^2 u + b \cdot \nabla u = f & \text{in } \Omega, \\ u = 0 & \text{on } \partial\Omega. \end{cases} \tag{2.1}$$

The data are specified as follows: $f \in L^2(\Omega)$ is a source term, $b \in L^\infty(\Omega; \mathbb{R}^d)$ is a drift coefficient, and $A \in L^\infty(\Omega; \mathbb{R}^{d\times d}_{\mathrm{sym}})$ is a uniformly elliptic diffusion coefficient, i.e.,

$$\exists\, \nu_1, \nu_2 > 0 \text{ s.t. } \forall \xi \in \mathbb{R}^d \backslash \{0\} : \quad \nu_1 \leq \frac{(A\xi)\cdot\xi}{\xi\cdot\xi} \leq \nu_2 \ \text{ a.e. in } \Omega. \tag{2.2}$$

Additionally, we assume that the pair (A, b) satisfies the Cordes-type condition

$$\exists\, \delta \in (\delta_0, 1] : \quad \frac{A : A + b \cdot b}{(\operatorname{tr}(A))^2} \leq \frac{1}{d - 1 + \delta} \quad \text{a.e. in } \Omega. \tag{2.3}$$

Here, the lower bound of admissible values for δ is given by

$$\delta_0 \coloneqq \frac{\eta}{1 + C_{\mathrm{P}}^2}, \qquad \eta \coloneqq \begin{cases} 1 & \text{if } \|b\|_{L^\infty} \neq 0, \\ 0 & \text{otherwise,} \end{cases} \tag{2.4}$$

where C_{P} is the Poincaré constant

$$C_{\mathrm{P}} \coloneqq \inf_{\varphi \in V \setminus \{0\}} \frac{\|D\varphi\|_{L^2}}{\|\varphi\|_{L^2}} > 0 \tag{2.5}$$

for the subspace V of $H^1(\Omega;\mathbb{R}^d)$ consisting of functions with vanishing tangential trace on $\partial\Omega$, that is,

$$V \coloneqq H^1_t(\Omega;\mathbb{R}^d) \coloneqq \big\{\varphi \in H^1(\Omega;\mathbb{R}^d) \ : \ \varphi - (\varphi \cdot n)n = 0 \text{ on } \partial\Omega\big\}, \tag{2.6}$$

where n denotes the exterior unit normal on $\partial\Omega$; see, e.g., [Bis88].

It is important to note that no regularity assumptions beyond L^∞ are imposed on the coefficients A and b. The scenario of particular interest here is when the coefficients are rough, with oscillations across multiple length scales.

2.1. **Well-posedness.** In the absence of a drift term b, condition (2.3) reduces to the classical Cordes condition introduced in [Cor56], which in two dimensions is already implied by the uniform ellipticity condition (2.2). In this case, it is well-known (cf. [Tal65, SS13]) that problem (2.1) admits a unique strong solution $u \in H^2(\Omega) \cap H^1_0(\Omega)$. When the drift term does not vanish, we can nevertheless establish existence and uniqueness of a strong solution to (2.1) under condition (2.3), using ideas from [SSZ25, Spr26]. To this end, we first introduce the notion of near operators as established by Campanato in [Cam94].

Lemma 2.1 (Campanato nearness)**.** *Let $L_1, L_2 \colon X \to Y$ be two maps from a set $X \neq \emptyset$ to a real Banach space $(Y, \|\cdot\|)$. Suppose that L_2 is bijective and that L_1 is (Campanato-)near L_2, that is, there exist constants $c > 0$ and $K \in [0,1)$ such that*

$$\forall v_1, v_2 \in X: \quad \|L_2(v_1) - L_2(v_2) - c\,[L_1(v_1) - L_1(v_2)]\,\| \leq K \|L_2(v_1) - L_2(v_2)\|.$$

Then, L_1 is bijective and we have the bound

$$\forall v_1, v_2 \in X: \quad \|L_2(v_1) - L_2(v_2)\| \leq \frac{c}{1-K} \|L_1(v_1) - L_1(v_2)\|. \tag{2.7}$$

Proof. We give a short proof for completeness. Since L_2 is bijective, we have that (X, ρ) is a nonempty complete metric space with the metric $\rho : X \times X \to [0,\infty)$ defined by $\rho(v_1, v_2) \coloneqq \|L_2(v_1) - L_2(v_2)\|$ for $v_1, v_2 \in X$. For $f \in Y$, we introduce

$$T_f : X \to X, \qquad T_f(v) \coloneqq L_2^{-1}(L_2(v) + c[f - L_1(v)]),$$

which is well-defined by bijectivity of L_2. We claim that T_f is a contraction on (X, ρ) for all $f \in Y$. Indeed, as L_1 is near L_2, we have for any $f \in Y$ and $v_1, v_2 \in X$ that

$$\rho(T_f(v_1), T_f(v_2)) = \|L_2(v_1) - L_2(v_2) - c\,[L_1(v_1) - L_1(v_2)]\,\| \leq K \rho(v_1, v_2).$$

Banach's fixed point theorem yields that for any $f \in Y$ there exists a unique $u \in X$ such that $T_f(u) = u$, i.e., $L_1(u) = f$. It follows that L_1 is bijective. Finally, for any $v_1, v_2 \in X$, we use the triangle inequality and the fact that L_1 is near L_2 to obtain the inequality $\rho(v_1, v_2) \leq c\|L_1(v_1) - L_1(v_2)\| + K\rho(v_1, v_2)$, which implies (2.7). □

We now introduce the renormalization function

$$\gamma \coloneqq \frac{\operatorname{tr}(A)}{A : A + b \cdot b} \in L^\infty(\Omega), \tag{2.8}$$

which is positive almost everywhere. The Cordes-type condition (2.3) then implies

$$(\gamma A - I_d) : (\gamma A - I_d) + (\gamma b) \cdot (\gamma b) = d - \gamma \operatorname{tr}(A) \leq 1 - \delta, \tag{2.9}$$

which allows us to show nearness of a renormalized version of the nondivergence-form differential operator

$$L \colon H^2(\Omega) \cap H^1_0(\Omega) \to L^2(\Omega), \qquad v \mapsto A : D^2 v + b \cdot \nabla v \tag{2.10}$$

to the Laplacian as established in the following lemma.

Lemma 2.2 (Nearness to the Laplacian)**.** *Let $\Omega \subset \mathbb{R}^d$ be a bounded convex domain, $A \in L^\infty(\Omega;\mathbb{R}^{d\times d}_{\mathrm{sym}})$, $b \in L^\infty(\Omega;\mathbb{R}^d)$, and suppose that* (2.2) *and* (2.3) *hold. Recall the constants $\delta, \delta_0, \eta, C_P$ from* (2.3), (2.4), *and* (2.5)*. Then, introducing the operator*

$$L_\gamma \colon H^2(\Omega)\cap H^1_0(\Omega) \to L^2(\Omega), \qquad v \mapsto \gamma A : D^2 v + \gamma b \cdot \nabla v \tag{2.11}$$

with $\gamma \in L^\infty(\Omega)$ given by (2.8)*, we have that*

$$\forall v \in H^2(\Omega)\cap H^1_0(\Omega): \quad \|\Delta v - L_\gamma v\|_{L^2} \le \sqrt{1-\kappa}\,\|\Delta v\|_{L^2},$$

where $\kappa \coloneqq (\delta-\delta_0)(1+\eta\, C_P^{-2}) \in (0,1]$. In particular,

$$L_\gamma : H^2(\Omega)\cap H^1_0(\Omega) \to L^2(\Omega) \quad \textit{is near} \quad \Delta : H^2(\Omega)\cap H^1_0(\Omega) \to L^2(\Omega)$$

in the sense of Campanato.

Proof. Let $v \in H^2(\Omega)\cap H^1_0(\Omega)$. Noting that $\nabla v \in V$ and using (2.5), we have that

$$C_{\mathrm{P}}\|\nabla v\|_{L^2} \le \|D^2 v\|_{L^2} \le \|\Delta v\|_{L^2},$$

where the second inequality is the Miranda–Talenti (or Kadlec) estimate. Together with (2.9), we then find that

$$\begin{aligned}\|\Delta v - L_\gamma v\|_{L^2}^2 &= \|(\gamma A - I_d) : D^2 v + \gamma b\cdot\nabla v\|_{L^2}^2 \\ &\le (1-\delta)\left(\|D^2 v\|_{L^2}^2 + \eta\,\|\nabla v\|_{L^2}^2\right) \\ &\le (1-\delta)\left(1+\eta\, C_{\mathrm{P}}^{-2}\right)\|\Delta v\|_{L^2}^2 = (1-\kappa)\|\Delta v\|_{L^2}^2,\end{aligned}$$

where $\kappa \coloneqq (\delta-\delta_0)(1+\eta\, C_P^{-2})$. Note that $\kappa \in (0,1]$ since $\delta \in (\delta_0, 1]$. □

We are now in a position to prove well-posedness of the nondivergence-form problem (2.1) by combining Lemmas 2.1 and 2.2.

Theorem 2.3 (Well-posedness of model problem)**.** *Let $\Omega \subset \mathbb{R}^d$ be a bounded convex domain, and $f \in L^2(\Omega)$. Let $A \in L^\infty(\Omega;\mathbb{R}^{d\times d}_{\mathrm{sym}})$ and $b \in L^\infty(\Omega;\mathbb{R}^d)$ be such that* (2.2) *and* (2.3) *hold. Then, there exists a unique solution $u \in H^2(\Omega)\cap H^1_0(\Omega)$ to* (2.1)*, and we have the bound*

$$\|\Delta u\|_{L^2} \le \frac{\|\gamma\|_{L^\infty}}{1-\sqrt{1-\kappa}}\,\|f\|_{L^2},$$

where $\gamma \in L^\infty(\Omega)$ is given by (2.8)*, and $\kappa \in (0,1]$ is defined in Lemma 2.2.*

Proof. We know from Lemma 2.2 that the operator $L_\gamma : H^2(\Omega)\cap H^1_0(\Omega) \to L^2(\Omega)$ given by (2.11) is near the bijective operator $\Delta : H^2(\Omega)\cap H^1_0(\Omega) \to L^2(\Omega)$ in the sense of Campanato (with $c=1$ and $K=\sqrt{1-\kappa}$). Hence, by Lemma 2.1, we find that $L_\gamma : H^2(\Omega)\cap H^1_0(\Omega) \to L^2(\Omega)$ is bijective and we have the bound

$$\forall v \in H^2(\Omega)\cap H^1_0(\Omega): \quad \|\Delta v\|_{L^2} \le \frac{1}{1-\sqrt{1-\kappa}}\,\|L_\gamma v\|_{L^2}.$$

Since $\gamma > 0$ almost everywhere in Ω and $L_\gamma = \gamma L$ with $L : H^2(\Omega)\cap H^1_0(\Omega) \to L^2(\Omega)$ given by (2.10), we find that L is bijective and we have the bound

$$\forall v \in H^2(\Omega)\cap H^1_0(\Omega): \quad \|\Delta v\|_{L^2} \le \frac{\|\gamma\|_{L^\infty}}{1-\sqrt{1-\kappa}}\,\|Lv\|_{L^2},$$

which yields the claimed result. □

2.2. **Symmetric Lax–Milgram problem for ∇u.** Our starting point for constructing a numerical homogenization method is the observation that, inspired by [Gal17, Gal19], ∇u can be characterized as the unique solution of a symmetric Lax–Milgram problem in the space V defined in (2.6).

For a chosen stabilization parameter $\sigma > 0$, we introduce the symmetric bilinear form $\mathfrak{a}\colon V \times V \to \mathbb{R}$ defined by

$$\mathfrak{a}(\psi,\varphi) \coloneqq (A : D\psi + b\cdot\psi, A : D\varphi + b\cdot\varphi)_{L^2} + \sigma\,(\mathrm{rot}(\psi),\mathrm{rot}(\varphi))_{L^2} \tag{2.12}$$

for $\psi, \varphi \in V$, where we used the notation

$$\mathrm{rot}(\psi) \coloneqq \begin{cases} \partial_2\psi_1 - \partial_1\psi_2, & \text{if } d = 2,\\ (\partial_2\psi_3 - \partial_3\psi_2,\ \partial_3\psi_1 - \partial_1\psi_3,\ \partial_1\psi_2 - \partial_2\psi_1), & \text{if } d = 3. \end{cases}$$

Then, we have the following result.

Lemma 2.4 (Characterization of ∇u)**.** *Let the setting be as in Theorem 2.3 with $d \in \{2,3\}$, and let $\sigma > 0$. Let $\mathfrak{a}\colon V \times V \to \mathbb{R}$ be the bilinear form given by* (2.12)*, and let $u \in H^2(\Omega) \cap H^1_0(\Omega)$ denote the unique strong solution to problem* (2.1)*. Then, the following assertions hold.*

(i) *Coercivity of $\mathfrak{a}$: there exists a constant $\alpha > 0$ such that for any $\varphi \in V$ it holds $\mathfrak{a}(\varphi,\varphi) \geq \alpha\|D\varphi\|^2_{L^2}$.*

(ii) *Boundedness of $\mathfrak{a}$: there exists a constant $\beta > 0$ such that for any $\psi, \varphi \in V$ it holds $|\mathfrak{a}(\psi,\varphi)| \leq \beta\|D\psi\|_{L^2}\|D\varphi\|_{L^2}$.*

(iii) *There exists a unique $z \in V$ such that*

$$\forall \varphi \in V: \quad \mathfrak{a}(z,\varphi) = (f, A : D\varphi + b\cdot\varphi)_{L^2}. \tag{2.13}$$

Moreover, it holds $z = \nabla u$.

Proof. (i) Let $\gamma \in L^\infty(\Omega)$ be the function defined in (2.8), and let $\kappa \in (0,1]$ be the constant defined in Lemma 2.2. Noting that $\sigma\|\gamma\|^2_{L^\infty} > 0$, we fix $\varepsilon > 0$ such that

$$\frac{1-\kappa}{\varepsilon} + \frac{(1-\sqrt{1-\kappa})^2}{1+\varepsilon} \leq \sigma\|\gamma\|^2_{L^\infty},$$

and we define the constants

$$r \coloneqq \frac{1-\kappa}{\varepsilon\|\gamma\|^2_{L^\infty}} \geq 0, \qquad \alpha \coloneqq \frac{(1-\sqrt{1-\kappa})^2}{(1+\varepsilon)\|\gamma\|^2_{L^\infty}} > 0.$$

For any $\varphi \in V$, writing $\tilde{L}\varphi \coloneqq A : D\varphi + b\cdot\varphi$ and noting that $\sigma \geq r + \alpha$, we have

$$\begin{aligned}
\mathfrak{a}(\varphi,\varphi) &\geq \|\tilde{L}\varphi\|^2_{L^2} + r\|\mathrm{rot}(\varphi)\|^2_{L^2} + \alpha\|\mathrm{rot}(\varphi)\|^2_{L^2}\\
&\geq \frac{\left[\|\tilde{L}\varphi\|_{L^2} + \sqrt{\varepsilon r}\,\|\mathrm{rot}(\varphi)\|_{L^2}\right]^2}{1+\varepsilon} + \alpha\|\mathrm{rot}(\varphi)\|^2_{L^2}\\
&\geq \frac{\left[\|\gamma\|_{L^\infty}\|\tilde{L}\varphi\|_{L^2} + \sqrt{1-\kappa}\,(\|D\varphi\|_{L^2} - \|\nabla\cdot\varphi\|_{L^2})\right]^2}{(1+\varepsilon)\|\gamma\|^2_{L^\infty}} + \alpha\|\mathrm{rot}(\varphi)\|^2_{L^2}\\
&\geq \frac{\left[\|\gamma\tilde{L}\varphi\|_{L^2} + \|\nabla\cdot\varphi - \gamma\tilde{L}\varphi\|_{L^2} - \sqrt{1-\kappa}\|\nabla\cdot\varphi\|_{L^2}\right]^2}{(1+\varepsilon)\|\gamma\|^2_{L^\infty}} + \alpha\|\mathrm{rot}(\varphi)\|^2_{L^2}\\
&\geq \alpha\|\nabla\cdot\varphi\|^2_{L^2} + \alpha\|\mathrm{rot}(\varphi)\|^2_{L^2}\\
&\geq \alpha\|D\varphi\|^2_{L^2},
\end{aligned}$$

where we have used the Maxwell (or Gaffney) estimate

$$\|D\varphi\|^2_{L^2} \leq \|\nabla\cdot\varphi\|^2_{L^2} + \|\mathrm{rot}(\varphi)\|^2_{L^2},$$

and in the third from last step that, by (2.9) and (2.5),

$$\begin{aligned}\|\gamma\tilde{L}\varphi - \nabla\cdot\varphi\|_{L^2}^2 &= \|(\gamma A - I_d) : D\varphi + \gamma b\cdot\varphi\|_{L^2}^2\\ &\le (1-\delta)\left(\|D\varphi\|_{L^2}^2 + \eta\|\varphi\|_{L^2}^2\right)\\ &\le (1-\delta)\left(1+\eta C_{\mathrm{P}}^{-2}\right)\|D\varphi\|_{L^2}^2 = (1-\kappa)\|D\varphi\|_{L^2}^2,\end{aligned}$$

with η given by (2.4).

(ii) This follows directly from Hölder's inequality, Poincaré's inequality (2.5), and the fact that $\|\mathrm{rot}(\varphi)\|_{L^2} \lesssim \|D\varphi\|_{L^2}$ for any $\varphi \in V$.

(iii) Note that $\|\cdot\|_V \coloneqq \|D(\cdot)\|_{L^2}$ defines a norm on V due to the Poincaré inequality (2.5). Therefore, in view of (i)-(ii), the Lax–Milgram theorem applies to yield the existence and uniqueness of a function $z \in V$ satisfying (2.13). Finally, since for the unique strong solution $u \in H^2(\Omega)\cap H_0^1(\Omega)$ to (2.1) we have that $\nabla u \in V$ and $\mathfrak{a}(\nabla u,\varphi) = (f, A : D\varphi + b\cdot\varphi)_{L^2}$ for any $\varphi \in V$ (as $A : D^2u + b\cdot\nabla u = f$ and $\mathrm{rot}(\nabla u) = 0$ almost everywhere in Ω), it follows that $z = \nabla u$ by the uniqueness of the solution to (2.13) in V. □

2.3. **Recovery of u.** Once the solution $z = \nabla u$ to (2.13) is computed, the recovery of u from z can be achieved as follows.

Lemma 2.5 (Recovery of u from z)**.** *Let the situation be as in Lemma 2.4. The solution $u \in H^2(\Omega)\cap H_0^1(\Omega)$ to (2.1) is the unique solution to the problem*

$$\begin{cases}\Delta u = \nabla\cdot z & \text{in } \Omega,\\ u = 0 & \text{on } \partial\Omega,\end{cases} \tag{2.14}$$

where $z \in V$ denotes the unique solution to (2.13).

Proof. The result follows directly from Lemma 2.4 (iii) together with the uniqueness of strong solutions to problem (2.14). □

3. Ideal numerical homogenization

In this section, we introduce an ideal numerical homogenization method that achieves optimal-order approximations without pre-asymptotic effects under minimal structural assumptions on the coefficients. Let $\Omega \subset \mathbb{R}^d$ be a bounded convex polyhedral domain in dimension $d \in \{2,3\}$, and consider a shape-regular hierarchy of geometrically conformal meshes $\{\mathcal{T}_H\}_{H>0}$ (cf. [EG04, Def. 1.55 & 1.107]). Each mesh $\mathcal{T}_H$ is a finite partition of $\overline{\Omega}$ into closed elements (either simplices or quadrilaterals/hexahedra). The mesh parameter $H > 0$ is defined by $H \coloneqq \max_{T\in\mathcal{T}_H}\mathrm{diam}(T)$. We assume that the family of meshes is quasi-uniform, that is, H can be bounded from above by a constant multiple of the minimal element diameter. We denote by $\mathcal{F}_H$ the set of all relatively closed mesh facets (edges for $d=2$, faces for $d=3$). To each facet $F \in \mathcal{F}_H$, we associate a fixed unit normal vector n_F.

3.1. **Fine-scale space.** A key ingredient in the numerical homogenization method considered here is the fine-scale space, consisting of functions that average out on coarse scales. This space is introduced via the concept of *quantities of interest*, which are associated with each facet $F \in \mathcal{F}_H$ and defined as

$$q_F \in V^*, \qquad \langle q_F, \varphi\rangle \coloneqq \int_F \varphi\cdot n_F \,\mathrm{d}s \quad \text{for } \varphi \in V. \tag{3.1}$$

The fine-scale space is then defined as the closed subspace given by the intersection of the kernels of these quantities of interest, that is,

$$W \coloneqq \bigcap_{F\in\mathcal{F}_H} \ker(q_F) \subset V. \tag{3.2}$$

The following lemma plays an essential role in the analysis of the method.

Lemma 3.1 (Local Poincaré-type inequality on W)**.** *There exists a constant $c_{\mathrm{p}} > 0$ independent of H such that, for all $T \in \mathcal{T}_H$, it holds that*

$$\forall w \in W: \quad \|w\|_{L^2(T)} \leq c_{\mathrm{p}} H \|Dw\|_{L^2(T)}. \tag{3.3}$$

Proof. This result can be derived from [EG04, Lem. B.66] using a transformation to the reference element and the corresponding estimates in [EG04, Lem. 1.101]. □

3.2. **Ideal method.** The problem-adapted approximation space of the ideal numerical homogenization method is defined as the orthogonal complement of W with respect to the energy inner product $\mathfrak{a}$, that is,

$$\tilde{V}_H \coloneqq \big\{ v \in V \,:\, \mathfrak{a}(v, w) = 0 \text{ for all } w \in W \big\}. \tag{3.4}$$

Since W has finite codimension in V, the space $\tilde{V}_H$ is finite-dimensional. The use of tildes emphasizes that these spaces are specifically adapted to the problem.

The prototypical LOD method is defined as the Galerkin projection onto the problem-adapted approximation space $\tilde{V}_H$; that is, it seeks $\tilde{z}_H \in \tilde{V}_H$ such that

$$\forall \tilde{v}_H \in \tilde{V}_H: \quad \mathfrak{a}(\tilde{z}_H, \tilde{v}_H) = (f, A : D\tilde{v}_H + b \cdot \tilde{v}_H)_{L^2}. \tag{3.5}$$

As will be seen later, both in theory (see Remark 3.3) and in numerical experiments, this method does not directly yield a convergence rate in terms of $\|D(z - \tilde{z}_H)\|_{L^2}$, where $z \in V$ denotes the unique solution to (2.13). To address this, we introduce additional corrections that allow us to extract rates from the right-hand side. To this end, let Y_H be a scalar-valued finite element space associated with the coarse mesh $\mathcal{T}_H$, and let $\Pi_H \colon H^1(\Omega) \to Y_H$ denote an interpolation operator satisfying, for some $p \in \mathbb{N}_0$, the following estimate

$$\forall k \in \{0, 1, \dots, p+1\}: \quad \|v - \Pi_H v\|_{L^2} \leq C_\Pi H^k |v|_{H^k} \text{ for all } v \in H^k(\Omega), \tag{3.6}$$

with a constant $C_\Pi > 0$ independent of H. Note that Y_H could, in principle, be replaced with any other space possessing approximation properties as in (3.6).

The correction operator $\mathcal{Q} \colon Y_H \to W$ is defined as follows: for any $y_H \in Y_H$, we define $\mathcal{Q} y_H \in W$ to be the unique element of W satisfying

$$\forall w \in W: \quad \mathfrak{a}(\mathcal{Q} y_H, w) = (y_H, A : Dw + b \cdot w)_{L^2}, \tag{3.7}$$

and the ideal approximation $\tilde{z}_H \in \tilde{V}_H$ satisfying (3.5) is then updated in a post-processing step, i.e.,

$$\hat{z}_H \coloneqq \tilde{z}_H + \mathcal{Q}(\Pi_H f), \tag{3.8}$$

assuming that $f \in H^1(\Omega)$.

Higher-order convergence rates, independent of the regularity of the coefficients and the solution, are established in the following theorem.

Theorem 3.2 (Ideal method)**.** *Suppose that $f \in H^{p+1}(\Omega)$. Let $z \in V$ denote the unique solution to* (2.13) *and let $\hat{z}_H$ be the post-processed ideal multiscale approximation as defined in* (3.8)*. Then, it holds*

$$\|D(z - \hat{z}_H)\|_{L^2} \leq \alpha^{-1} \big(\|A\|_{L^\infty} + C_{\mathrm{P}}^{-1} \|b\|_{L^\infty} \big) C_\Pi H^{p+1} |f|_{H^{p+1}}, \tag{3.9}$$

$$\|z - \hat{z}_H\|_{L^2} \leq c_{\mathrm{P}} H \|D(z - \hat{z}_H)\|_{L^2}, \tag{3.10}$$

where $\alpha > 0$ is the coercivity constant for $\mathfrak{a}$ from Lemma 2.4, $C_{\mathrm{P}}, c_{\mathrm{P}} > 0$ are the Poincaré constants from (2.5) *and* (3.3)*, and $C_\Pi > 0$ is the interpolation constant from* (3.6)*.*

Proof. We use the coercivity of $\mathfrak{a}$ from Lemma 2.4, the definition of $\mathcal{Q}$ in (3.7), and the observation that $z - \hat{z}_H = z - \tilde{z}_H - \mathcal{Q}(\Pi_H f) \in W$ to obtain

$$\begin{aligned}\alpha\|D(z-\hat{z}_H)\|_{L^2}^2 &\le \mathfrak{a}(z-\tilde{z}_H-\mathcal{Q}(\Pi_H f), z-\hat{z}_H)\\ &= (f-\Pi_H f, A : D(z-\hat{z}_H) + b\cdot(z-\hat{z}_H))_{L^2}\\ &\le (\|A\|_{L^\infty}\|D(z-\hat{z}_H)\|_{L^2} + \|b\|_{L^\infty}\|z-\hat{z}_H\|_{L^2})\,\|f-\Pi_H f\|_{L^2}.\end{aligned}$$

In view of the Poincaré inequality (2.5), we find that

$$\|D(z-\hat{z}_H)\|_{L^2} \le \alpha^{-1}\left(\|A\|_{L^\infty} + C_{\mathrm{P}}^{-1}\|b\|_{L^\infty}\right)\|f-\Pi_H f\|_{L^2}.$$

The estimate (3.9) then follows using the interpolation error bound (3.6). Finally, since $z - \hat{z}_H \in W$, the L^2-estimate (3.10) is a consequence of (3.9) in view of Lemma 3.1. □

Note that the variant (3.8) does not require f to be known. It just requires to compute a set of additional corrections that are based on a low-dimensional space in which f may be suitably approximated. This slightly increased complexity regarding number of corrections makes it possible to obtain rates for the ideal method of essentially any order (depending on the amount of additional corrections and the corresponding spaces). This approach has some similarities to the enriched multiscale construction in [KKMW25] (to capture time-dependence) and the right-hand side corrections in [HM17]. However, the latter requires f to be known.

Let us briefly comment on the necessity of correcting the ideal approximation $\tilde{z}_H$ as done in (3.8).

Remark 3.3 (Necessity of a correction). Noting that $z-\tilde{z}_H \in W$, and recalling (3.2) and (3.4), an analogous argument to [AHP21, Thm. 3.9] yields the bound

$$\begin{aligned}\|D(z-\tilde{z}_H)\|_{L^2} &\le \alpha^{-1}\inf_{\{c_F\}_F\subset\mathbb{R}}\sup_{w\in W\setminus\{0\}}\frac{\mathfrak{a}(z-\tilde{z}_H,w)-\sum_{F\in\mathcal{F}_H}c_F\langle q_F,w\rangle}{\|Dw\|_{L^2}}\\ &= \alpha^{-1}\inf_{\{c_F\}\subset\mathbb{R}}\sup_{w\in W\setminus\{0\}}\frac{(f,A:Dw+b\cdot w)_{L^2}-\sum_{F\in\mathcal{F}_H}c_F\langle q_F,w\rangle}{\|Dw\|_{L^2}},\end{aligned}$$

which reveals no convergence rate without an additional correction.

3.3. **Alternative characterization of $\tilde{V}_H$.** To better understand the structure of the space $\tilde{V}_H$, we characterize the $\mathfrak{a}$-orthogonal projection $\mathcal{R}\colon V \to \tilde{V}_H$ via a saddle point formulation. This formulation uses Lagrange multipliers defined on the mesh skeleton $\Sigma \coloneqq \bigcup_{F\in\mathcal{F}_H} F$ in the space

$$M_H \coloneqq \{v \in L^2(\Sigma) \,:\, v|_F = \text{const} \ \text{ for all } F \in \mathcal{F}_H\}.$$

Specifically, for any $v \in V$, the projection $\mathcal{R}v \in V$ and the associated Lagrange multiplier $\lambda \in M_H$ are defined as the unique solution pair to

$$\mathfrak{a}(\mathcal{R}v, w) + \mathfrak{b}(w,\lambda) = 0 \qquad \text{for all } w \in V, \tag{3.11a}$$

$$\mathfrak{b}(\mathcal{R}v, \mu) = \mathfrak{b}(v,\mu) \qquad \text{for all } \mu \in M_H, \tag{3.11b}$$

where $\mathfrak{b}$ denotes the bilinear form

$$\mathfrak{b}\colon V\times M_H\to\mathbb{R}, \qquad \mathfrak{b}(v,\mu) \coloneqq \sum_{F\in\mathcal{F}_H}\int_F (v\cdot n_F)\mu\,\mathrm{d}s.$$

Indeed, equation (3.11a) ensures that $\mathcal{R}v \in \tilde{V}_H$, while equation (3.11b) implies that $\mathcal{R}v - v \in W$. The well-posedness of (3.11) then follows from classical saddle point theory (cf. [BBF13, Cor. 4.2.1]) and, in particular, relies on the inf–sup condition

$$\inf_{\mu\in M_H\setminus\{0\}}\sup_{v\in V\setminus\{0\}}\frac{\mathfrak{b}(v,\mu)}{\|Dv\|_{L^2(\Omega)}\|\mu\|_{L^2(\Sigma)}} \gtrsim H^{1/2} > 0. \tag{3.12}$$

This inf–sup condition can be proved using bubble functions $\{\rho_F : F \in \mathcal{F}_H\}$ such that $\rho_F \in V$ with $\operatorname{supp}(\rho_F) \subset \omega_F$, where ω_F denotes the union of the elements sharing the facet F (one for boundary facets and two for interior facets). These bubble functions can be chosen such that

$$\forall F, F' \in \mathcal{F}_H : \quad \langle q_{F'}, \rho_F \rangle = \delta_{F'F}, \tag{3.13}$$

and such that the following stability estimates are satisfied:

$$\|\rho_F\|_{L^2(\omega_F)} \lesssim H^{-d/2+1}, \qquad \|D\rho_F\|_{L^2(\omega_F)} \lesssim H^{-d/2}. \tag{3.14}$$

To prove the inf–sup condition (3.12), we construct, for any given $\mu \in M_H$, a function $v \in V$ that possesses the same quantities of interest, by

$$v \coloneqq \sum_{F \in \mathcal{F}_H} \mu|_F \rho_F,$$

where ρ_F are the bubble functions introduced above. Noting that, by construction, we have $\mathfrak{b}(v,\mu) = |\mu|^2$ with $|\mu|^2 \coloneqq \sum_{F\in\mathcal{F}_H}(\mu|_F)^2$, and employing the locality of the bubble functions and the stability estimates from (3.14), we obtain

$$\|Dv\|_{L^2}^2 \lesssim \sum_{F\in\mathcal{F}_H} (\mu|_F)^2 \|D\rho_F\|_{L^2(\omega_F)}^2 \lesssim H^{-d}|\mu|^2.$$

Combining these estimates, and noting that $\|\mu\|_{L^2(\Sigma)}^2 \lesssim H^{d-1}|\mu|^2$, we deduce the inf–sup stability bound (3.12).

4. Exponential decay

In this section, we prove exponential decay properties of the operator $\mathcal{R} : V \to \tilde{V}_H$ defined in (3.11), as well as of related operators. These decay properties will then allow us to define a localized version of $\mathcal{R}$ in Section 5 and to construct a practical numerical homogenization method with locally computable basis functions in Section 6. To quantify this decay behavior, we introduce the concept of patches. Given an *oversampling parameter* $\ell \in \mathbb{N}$, the ℓ-th order patch of a union of elements $S \subset \mathcal{T}_H$ is defined recursively for $\ell \geq 2$ by $\mathsf{N}^\ell(S) \coloneqq \mathsf{N}^1(\mathsf{N}^{\ell-1}(S))$, where $\mathsf{N}^1(S) \coloneqq \mathsf{N}(S)$ denotes the set of mesh elements sharing at least one node with the elements in S. We set $\mathsf{N}^0(S) \coloneqq S$.

Theorem 4.1 (Exponential decay)**.** *Let $S \subset \mathcal{T}_H$ be a union of mesh elements, and let $(\psi,\lambda) \in V \times M_H$ be the unique solution to the problem*

$$\mathfrak{a}(\psi,v) + \mathfrak{b}(v,\lambda) = f_S(v) \quad \text{for all } v \in V, \tag{4.1a}$$

$$\mathfrak{b}(\psi,\mu) = g_S(\mu) \quad \text{for all } \mu \in M_H, \tag{4.1b}$$

where $f_S \in V^*$ and $g_S \in (M_H)^*$ are such that $f_S(v) = 0$ for all $v \in V$ with $\operatorname{supp}(v) \subset \overline{\Omega \setminus S}$, and $g_S(\mu) = 0$ for all $\mu \in M_H$ with $\operatorname{supp}(\mu) \subset \overline{\Omega \setminus S}$. Then, there exists a constant $c > 0$, independent of H, ℓ, and S, such that

$$\|D\psi\|_{L^2(\Omega\setminus\mathsf{N}^\ell(S))} \leq \exp(-c\ell)\, \|D\psi\|_{L^2}$$

for all $\ell \in \mathbb{N}$.

Proof. The proof relies on cut-off techniques, which are widely used in the context of multiscale methods (see, e.g., [MP20, AHP21]) and are adapted here to the present setting. We fix an integer $\ell \geq 1$ and denote by $\eta \in W^{1,\infty}(\Omega)$ the first-order Lagrange finite element cut-off function, defined with respect to $\mathcal{T}_H$, characterized by

$$\eta = 0 \text{ in } \mathsf{N}^{\ell-1}(S), \quad \eta = 1 \text{ in } \Omega \setminus \mathsf{N}^\ell(S), \tag{4.2}$$

with the transition region $R \coloneqq \mathsf{N}^\ell(S) \setminus \mathsf{N}^{\ell-1}(S)$. It satisfies

$$\|\nabla\eta\|_{L^\infty} \lesssim H^{-1}. \tag{4.3}$$

We have that

$$\begin{aligned}
\|D\psi\|^2_{L^2(\Omega\setminus N^\ell(S))} &\le \|D(\eta\psi)\|^2_{L^2} \\
&\lesssim \mathfrak{a}(\eta\psi,\eta\psi) \\
&= \mathfrak{a}(\psi,\eta\psi) - \mathfrak{a}((1-\eta)\psi,\eta\psi) \\
&= f_S(\eta\psi) - \mathfrak{b}(\eta\psi,\lambda) - \mathfrak{a}((1-\eta)\psi,\eta\psi) \\
&=: \Xi_1 - \Xi_2 - \Xi_3.
\end{aligned}$$

Note that $\Xi_1 = 0$ since $\operatorname{supp}(\eta\psi) \subset \overline{\Omega \setminus N^{\ell-1}(S)} \subset \overline{\Omega \setminus S}$.

In order to bound the term Ξ_2, let us first recall the trace inequality

$$\forall v \in H^1(T_F;\mathbb{R}^d): \quad \|v\|_{L^2(F)} \lesssim H^{-1/2}\|v\|_{L^2(T_F)} + H^{1/2}\|Dv\|_{L^2(T_F)}, \tag{4.4}$$

where T_F denotes an element such that $F \subset T_F$; see, e.g., [DPE11, Lem. 1.49]. To estimate $\lambda|_F$, we obtain by testing (4.1a) with the bubble function ρ_F for each face $F \subset R$ (recall (3.13), (3.14), and note $\operatorname{supp}(\rho_F) \subset \omega_F \subset \overline{\Omega \setminus S}$) that

$$\begin{aligned}
|\lambda|_F| = |\mathfrak{b}(\rho_F,\lambda)| &= |\mathfrak{a}(\psi,\rho_F)| \\
&\lesssim \big(\|D\rho_F\|_{L^2(\omega_F)} + \|\rho_F\|_{L^2(\omega_F)}\big)\big(\|D\psi\|_{L^2(\omega_F)} + \|\psi\|_{L^2(\omega_F)}\big) \\
&\lesssim H^{-d/2}\|D\psi\|_{L^2(\omega_F)},
\end{aligned}$$

using the local Poincaré inequality from Lemma 3.1 and the bound (3.14) in the final step. Since $\langle q_F,\psi\rangle = 0$ for all faces F outside $\operatorname{int}(S)$ by (4.1b), we have

$$\Xi_2 = \sum_{F\in\mathcal{F}_H\,:\,F\subset R}\int_F (\eta\psi\cdot n_F)\,\lambda|_F\,\mathrm{d}s \lesssim \sum_{F\in\mathcal{F}_H\,:\,F\subset R}\|D\psi\|^2_{L^2(\omega_F)} \lesssim \|D\psi\|^2_{L^2(R)},$$

where we have used Lemma 3.1 and the trace inequality (4.4).

Finally, we estimate the term Ξ_3. We have

$$\begin{aligned}
\Xi_3 &\lesssim \big(\|D((1-\eta)\psi)\|_{L^2(R)} + \|(1-\eta)\psi\|_{L^2(R)}\big)\big(\|D(\eta\psi)\|_{L^2(R)} + \|\eta\psi\|_{L^2(R)}\big) \\
&\lesssim \|D\psi\|^2_{L^2(R)},
\end{aligned}$$

where we used the product rule, the bound (4.3) for the cut-off function, and Lemma 3.1.

Since $R = (\Omega \setminus \mathsf{N}^{\ell-1}(S)) \setminus (\Omega \setminus \mathsf{N}^\ell(S))$, we conclude that for a constant $C > 0$ independent of H and ℓ, it holds that

$$\|D\psi\|^2_{L^2(\Omega\setminus\mathsf{N}^\ell(S))} \le C\|D\psi\|^2_{L^2(R)} = C\|D\psi\|^2_{L^2(\Omega\setminus\mathsf{N}^{\ell-1}(S))} - C\|D\psi\|^2_{L^2(\Omega\setminus\mathsf{N}^\ell(S))},$$

which, after rearranging the terms, leads to

$$\|D\psi\|^2_{L^2(\Omega\setminus\mathsf{N}^\ell(S))} \le \frac{C}{1+C}\,\|D\psi\|^2_{L^2(\Omega\setminus\mathsf{N}^{\ell-1}(S))}.$$

Iterating the argument gives the assertion with decay rate $c \coloneqq \frac{1}{2}\log\big(\frac{1+C}{C}\big)$. □

5. Localization

To localize the operator $\mathcal{R}$, we follow the approach proposed in the recent generalized framework for high-order LOD methods [HLM26], which has also been applied in [HL25a, HMM25]. This framework enables a stable basis construction, ensuring that the error of the localized method does not grow as the coarse mesh is refined, provided that the oversampling parameter, defined as the number of element layers forming the oversampling domains, remains fixed. Such undesirable effects have been observed, for example, in [MP14, Mai21]. Notably, this stability

is achieved without relying on intricate bubble function constructions in practical implementations of the method (cf. [HP22a, DHM23]).

The key idea of this localization approach is to expresses the operator $\mathcal{R}$ as

$$\mathcal{R} = \mathcal{I}_H - \mathcal{K}, \tag{5.1}$$

where the operator $\mathcal{K}\colon V \to V$ will be characterized below, and $\mathcal{I}_H\colon V \to V_H$ is a quasi-interpolation operator onto the first-order V-conforming finite element space V_H associated with the mesh $\mathcal{T}_H$. The quasi-interpolation operator $\mathcal{I}_H$ (which is not necessarily a projection) is assumed to satisfy classical local approximation and stability estimates. That is, for all elements $T \in \mathcal{T}_H$, we have

$$\forall v \in V: \quad H^{-1}\|v - \mathcal{I}_H v\|_{L^2(T)} + \|D(\mathcal{I}_H v)\|_{L^2(T)} \lesssim \|Dv\|_{L^2(\mathsf{N}(T))}. \tag{5.2}$$

Moreover, $\mathcal{I}_H$ should depend on its argument only through its quantities of interest defined in (3.1), i.e., $\mathcal{I}_H w = 0$ for all $w \in W$. Operators with these properties can be readily constructed for the problem at hand. A detailed description of such a construction is provided in Section 7.

The operator $\mathcal{K}\colon V \to V$, as introduced in (5.1), is characterized for each $v \in V$ via the unique solution $(\mathcal{K}v, \lambda) \in V \times M_H$ to the saddle point problem

$$\begin{aligned}
&\mathfrak{a}(\mathcal{K}v, w) + \mathfrak{b}(w, \lambda) = \mathfrak{a}(\mathcal{I}_H v, w) && \text{for all } w \in V, && \text{(5.3a)}\\
&\mathfrak{b}(\mathcal{K}v, \mu) = -\mathfrak{b}(v - \mathcal{I}_H v, \mu) && \text{for all } \mu \in M_H. && \text{(5.3b)}
\end{aligned}$$

We note that if $(\mathcal{K}v, \lambda)$ is the solution to (5.3), then $((\mathcal{I}_H - \mathcal{K})v, -\lambda)$ is the solution to (3.11). The operator $\mathcal{K}$ can be expressed as a sum of local element contributions, i.e.,

$$\mathcal{K} = \sum_{T \in \mathcal{T}_H} \mathcal{K}_T,$$

where, for each $T \in \mathcal{T}_H$, the operator $\mathcal{K}_T\colon V \to V$ is defined, for $v \in V$, via the unique solution $(\mathcal{K}_T v, \lambda_T) \in V \times M_H$ to the modified saddle point problem

$$\begin{aligned}
&\mathfrak{a}(\mathcal{K}_T v, w) + \mathfrak{b}(w, \lambda_T) = \mathfrak{a}_T(\mathcal{I}_H v, w) && \text{for all } w \in V, && \text{(5.4a)}\\
&\mathfrak{b}(\mathcal{K}_T v, \mu) = -\mathfrak{b}_T(v - \mathcal{I}_H v, \mu) && \text{for all } \mu \in M_H. && \text{(5.4b)}
\end{aligned}$$

Here, for $T \in \mathcal{T}_H$, The bilinear form $\mathfrak{b}_T$ denotes a localized version of $\mathfrak{b}$ defined as

$$\mathfrak{b}_T(v, \mu) \coloneqq \sum_{F \in \mathcal{F}_H\,:\,F \subset \partial T} \frac{1}{N(F)}\, \mu|_F\, \langle q_F, v\rangle,$$

where $N(F) \coloneqq \#\{K \in \mathcal{T}_H \,:\, F \subset \partial K\}$ is the number of elements sharing the face $F \in \mathcal{F}_H$. The localized version $\mathfrak{a}_T$ of the bilinear form $\mathfrak{a}$ is defined by restricting the domain of integration in (2.12) to the element T.

Due to the general setting considered in Theorem 4.1, the result applies to the function $\mathcal{K}_T v$ for any $v \in V$, and shows that it decays exponentially away from the element T. This motivates the localization of the operator $\mathcal{K}_T$ to ℓ-th order patches around T. To this end, we introduce the corresponding localized spaces

$$\begin{aligned}
V_T^\ell &\coloneqq \big\{v \in V \,:\, v = 0 \text{ a.e. in } \Omega \setminus \mathsf{N}^\ell(T)\big\},\\
M_T^\ell &\coloneqq \big\{\mu \in M_H \,:\, \mu|_F = 0 \text{ for all } F \in \mathcal{F}_H \setminus \mathcal{F}_T^\ell\big\},
\end{aligned} \tag{5.5}$$

where $\mathcal{F}_T^\ell \subset \mathcal{F}_H$ denotes the localized set of facets, defined by

$$\mathcal{F}_T^\ell \coloneqq \big\{F \in \mathcal{F}_H \,:\, F \subset \mathsf{N}^\ell(T) \text{ and } F \setminus \partial\mathsf{N}^\ell(T) \neq \emptyset\big\}.$$

The localized operator $\mathcal{K}_T^\ell\colon V \to V_T^\ell$ can then be defined, for any $v \in V$, as the unique solution $(\mathcal{K}_T^\ell v, \lambda_T^\ell) \in V_T^\ell \times M_T^\ell$ to the local saddle point problem

$$\begin{aligned}
&\mathfrak{a}(\mathcal{K}_T^\ell v, w) + \mathfrak{b}(w, \lambda_T^\ell) = \mathfrak{a}_T(\mathcal{I}_H v, w) && \text{for all } w \in V_T^\ell, && \text{(5.6a)}\\
&\mathfrak{b}(\mathcal{K}_T^\ell v, \mu) = -\mathfrak{b}_T(v - \mathcal{I}_H v, \mu) && \text{for all } \mu \in M_T^\ell. && \text{(5.6b)}
\end{aligned}$$

Finally, a localized version of the operator $\mathcal{R}$ can be defined by

$$\mathcal{R}^\ell \coloneqq \mathcal{I}_H - \mathcal{K}^\ell, \qquad \mathcal{K}^\ell \coloneqq \sum_{T\in\mathcal{T}_H} \mathcal{K}_T^\ell. \tag{5.7}$$

The following theorem shows that the localized operator $\mathcal{R}^\ell$ approximates $\mathcal{R}$ exponentially well in the operator norm. Notably, it avoids the H^{-1} pre-factor typically arising in naive localization strategies (see, e.g., [MP14, Mai21]) while also avoiding technical bubble constructions as in [DHM23] in the implementation.

Theorem 5.1 (Localization error for $\mathcal{R}$)**.** *For all $v \in V$ and $\ell \in \mathbb{N}$, we have*

$$\|D(\mathcal{R}v - \mathcal{R}^\ell v)\|_{L^2} \lesssim \ell^{(d-1)/2}\exp(-c\ell)\|Dv\|_{L^2},$$

where $c > 0$ is the constant from Theorem 4.1.

Proof. The proof, which is an adaptation of that of [HLM26, Thm. 5.1] to the present setting, is included for completeness. We abbreviate the localization error by $e \coloneqq (\mathcal{R}-\mathcal{R}^\ell)v$ and note that $e \in W$. Indeed, by (5.4b), (5.1), (5.7), and (5.6b), we obtain $\mathfrak{b}(e,\mu) = 0$ for all $\mu \in M_H$. Here we used that $b(\mathcal{K}_T^\ell v,\mu) = b(\mathcal{K}_T^\ell v, \mu|_{\mathcal{F}_T^\ell})$ for all $\mu \in M_H$, which follows from the definitions of V_T^ℓ and M_T^ℓ in (5.5). We interpret $\mu|_{\mathcal{F}_T^\ell}$ as the restriction to the union of all facets in $\mathcal{F}_T^\ell$. Thus,

$$\alpha\|De\|_{L^2}^2 \le \mathfrak{a}(e,e) = -\mathfrak{a}(\mathcal{R}^\ell v, e) = \sum_{T\in\mathcal{T}_H}\Big(-\mathfrak{a}_T(\mathcal{I}_H v, e) + \mathfrak{a}(\mathcal{K}_T^\ell v, e)\Big). \tag{5.8}$$

In the following, we estimate each term in the summation on the right hand side separately. Let $\eta_T \in W^{1,\infty}(\Omega)$ denote the cut-off function from (4.2) with $S = T$. Noting that $\eta_T = 0$ on T, and using (5.6a) with the test function $w = (1-\eta_T)e \in V_T^\ell$, we find

$$\begin{aligned}-\mathfrak{a}_T(\mathcal{I}_H v, e) + \mathfrak{a}(\mathcal{K}_T^\ell v, e) &= -\mathfrak{a}_T(\mathcal{I}_H v, (1-\eta_T)e) + \mathfrak{a}(\mathcal{K}_T^\ell v, (1-\eta_T)e + \eta_T e)\\ &= -\mathfrak{b}((1-\eta_T)e, \lambda_T^\ell) + \mathfrak{a}(\mathcal{K}_T^\ell v, \eta_T e) =: \Theta_1 + \Theta_2.\end{aligned}$$

To estimate the term Θ_1, we decompose $\lambda_T^\ell = \lambda_T^{\mathrm{in}} + \lambda_T^{\mathrm{out}}$, where

$$\lambda_T^{\mathrm{in}} = \lambda_T^\ell|_{\mathcal{F}_T^{\ell-1}}, \qquad \lambda_T^{\mathrm{out}} = \lambda_T^\ell|_{\mathcal{F}_H\setminus\mathcal{F}_T^{\ell-1}},$$

both extended by zero to all other facets so that $\lambda_T^{\mathrm{in}}, \lambda_T^{\mathrm{out}} \in M_H$. Since $\eta_T = 0$ in $\mathsf{N}^{\ell-1}(T)$, we have that $\mathfrak{b}((1-\eta_T)e,\lambda_T^{\mathrm{in}}) = \mathfrak{b}(e,\lambda_T^{\mathrm{in}}) = 0$ by (5.4b) and (5.6b). Thus, with $R_T \coloneqq \operatorname{int}\big(\mathsf{N}^\ell(T)\setminus\mathsf{N}^{\ell-1}(T)\big)$, we obtain with the same arguments as for Ξ_2 in the proof of Theorem 4.1 that

$$\begin{aligned}\Theta_1 &= -\mathfrak{b}((1-\eta_T)e,\lambda_T^{\mathrm{out}})\\ &= -\sum_{F\in\mathcal{F}_H\,:\,F\subset R_T}\int_F (1-\eta_T)e\cdot n_F\lambda_T^{\mathrm{out}}\,\mathrm{d}s\\ &\lesssim \|D(\mathcal{K}_T^\ell v)\|_{L^2(R_T)}\|De\|_{L^2(R_T)}.\end{aligned}$$

Turning to $\Theta_2 = \mathfrak{a}(\mathcal{K}_T^\ell v, \eta_T e)$, we remark that the element contributions to this term also vanish for all the mesh elements outside R_T. As above, we arrive at

$$\Theta_2 \lesssim \|D(\mathcal{K}_T^\ell v)\|_{L^2(R_T)}\big(\|De\|_{L^2(R_T)} + \|e\|_{L^2(R_T)}\big) \lesssim \|D(\mathcal{K}_T^\ell v)\|_{L^2(R_T)}\|De\|_{L^2(R_T)}.$$

Combining the estimates for Θ_1 and Θ_2, we obtain

$$\begin{aligned}\|De\|_{L^2}^2 &\lesssim \sum_{T\in\mathcal{T}_H}\|D(\mathcal{K}_T^\ell v)\|_{L^2(R_T)}\|De\|_{L^2(R_T)}\\ &\lesssim \exp(-c\ell)\sum_{T\in\mathcal{T}_H}\|D(\mathcal{K}_T^\ell v)\|_{L^2(\mathsf{N}^\ell(T))}\|De\|_{L^2(R_T)},\end{aligned} \tag{5.9}$$

where we have applied Theorem 4.1 to (5.6), treating the patch $\mathsf{N}^\ell(T)$ as the whole domain. To pass from the norm of $\mathcal{K}_T^\ell v$ to that of v, we again use classical saddle point theory (see, e.g., [BBF13, Cor. 4.2.1]), noting that the inf–sup constant of $\mathfrak{b}$ for the pair (V_T^ℓ, M_T^ℓ) is of order $H^{1/2}$ following the arguments in (3.12). Hence,

$$\begin{aligned}\|D(\mathcal{K}_T^\ell v)\|_{L^2(\mathsf{N}^\ell(T))} &\lesssim \sup_{w\in V_T^\ell\setminus\{0\}} \frac{\mathfrak{a}_T(\mathcal{I}_H v, w)}{\|Dw\|_{L^2}} + H^{-1/2} \sup_{\mu\in M_T^\ell\setminus\{0\}} \frac{\mathfrak{b}_T(v-\mathcal{I}_H v,\mu)}{\|\mu\|_{L^2(\Sigma)}}\\ &\lesssim \|v\|_{H^1(\mathsf{N}(T))}\end{aligned}$$

where, in the last step, to estimate the first term involving $\mathfrak{a}_T$, we used the L^∞-bounds on the coefficients A and b, the properties of $\mathcal{I}_H$ as stated in (5.2), and the Poincaré inequality for w, cf. (2.5). The second term involving $\mathfrak{b}_T$ is treated analogously, additionally invoking the classical trace inequality from (4.4).

Returning to (5.9), we conclude that

$$\begin{aligned}\|De\|_{L^2}^2 &\lesssim \exp(-c\ell)\sqrt{\sum_{T\in\mathcal{T}_H}\|v\|_{H^1(\mathsf{N}(T))}^2}\sqrt{\sum_{T\in\mathcal{T}_H}\|De\|_{L^2(R_T)}^2}\\ &\lesssim \ell^{(d-1)/2}\exp(-c\ell)\|Dv\|_{L^2}\|De\|_{L^2},\end{aligned}$$

where we have used the fact that each element $K\in\mathcal{T}_H$ belongs to at most $\mathcal{O}(\ell^{d-1})$ rings R_T for different $T\in\mathcal{T}_H$, as well as the Poincaré inequality for v, cf. (2.5). Dividing by $\|De\|_{L^2}$ yields the assertion. □

The remainder of this section is devoted to the localization of the operator $\mathcal{Q}\colon Y_H\to W$ defined in (3.7). As above, for a given $y_H\in Y_H$, the function $\mathcal{Q}y_H$ is characterized by the solution pair $(\mathcal{Q}y_H,\zeta)\in V\times M_H$ satisfying

$$\begin{aligned}\mathfrak{a}(\mathcal{Q}y_H, w) \quad+\quad \mathfrak{b}(w,\zeta) &= (y_H, A:Dw + b\cdot w)_{L^2} && \text{for all } w\in V,\\ \mathfrak{b}(\mathcal{Q}y_H,\mu) &= 0 && \text{for all } \mu\in M_H.\end{aligned}$$

For any $T\in\mathcal{T}_H$, we define the corresponding element contributions $(\mathcal{Q}_T y_H,\zeta_T)\in V\times M_H$ as the solution to

$$\begin{aligned}\mathfrak{a}(\mathcal{Q}_T y_H, w) \quad+\quad \mathfrak{b}(w,\zeta_T) &= (y_H, A:Dw + b\cdot w)_{L^2(T)} && \text{for all } w\in V,\\ \mathfrak{b}(\mathcal{Q}_T y_H,\mu) &= 0 && \text{for all } \mu\in M_H.\end{aligned}$$

Note that $\mathcal{Q}=\sum_{T\in\mathcal{T}_H}\mathcal{Q}_T$. Moreover, the operators $\mathcal{Q}_T$ exhibit exponential decay away from T, as a direct consequence of Theorem 4.1. Their localized counterparts are obtained from the solution pair $(\mathcal{Q}_T^\ell y_H,\zeta_T^\ell)\in V_T^\ell\times M_T^\ell$ to

$$\begin{aligned}&\text{(5.12a)}\quad \mathfrak{a}(\mathcal{Q}_T^\ell y_H, w) \quad+\mathfrak{b}(w,\zeta_T^\ell) = (y_H, A:Dw+b\cdot w)_{L^2(T)} && \text{for all } w\in V_T^\ell,\\ &\text{(5.12b)}\quad \mathfrak{b}(\mathcal{Q}_T^\ell y_H,\mu) = 0 && \text{for all } \mu\in M_T^\ell.\end{aligned}$$

For the localized version $\mathcal{Q}^\ell\coloneqq\sum_{T\in\mathcal{T}_H}\mathcal{Q}_T^\ell$ of the operator $\mathcal{Q}$, the following exponential approximation result holds.

Theorem 5.2 (Localization error for $\mathcal{Q}$)**.** *For all $y_H\in Y_H$ and $\ell\in\mathbb{N}$, we have*

$$\|D(\mathcal{Q}y_H-\mathcal{Q}^\ell y_H)\|_{L^2}\lesssim \ell^{(d-1)/2}\exp(-c\ell)\|y_H\|_{L^2},$$

where $c>0$ is the constant from Theorem 4.1.

Proof. The proof is very similar to the proof of Theorem 5.1 and is therefore reduced to the essential steps. The missing precise arguments are exactly as in the above proof. Let $e\coloneqq(\mathcal{Q}-\mathcal{Q}^\ell)y_H$. With the cut-off function from (4.2) with $S=T$, now denoted by η_T, we obtain

$$\alpha\|De\|_{L^2}^2\le\mathfrak{a}((\mathcal{Q}-\mathcal{Q}^\ell)y_H,e)=(y_H,A:De+b\cdot e)_{L^2}-\mathfrak{a}(\mathcal{Q}^\ell y_H,e)$$

$$
\begin{aligned}
&= \sum_{T\in\mathcal{T}_H} \Big(- \mathfrak{a}(\mathcal{Q}_T^\ell y_H, (1-\eta_T)e + \eta_T e) \\
&\qquad\qquad + (y_H, A : D[(1-\eta_T)e] + b\cdot(1-\eta_T)e)_{L^2(T)}\Big) \\
&= \sum_{T\in\mathcal{T}_H} \mathfrak{b}((1-\eta_T)e, \zeta_T^\ell|_{\Sigma\setminus\mathsf{N}^{\ell-1}(T)}) - \mathfrak{a}(\mathcal{Q}_T^\ell y_H, \eta_T e) \\
&\lesssim \sum_{T\in\mathcal{T}_H} \|D(\mathcal{Q}_T^\ell y_H)\|_{L^2(R_T)}\|De\|_{L^2(R_T)} \\
&\lesssim \exp(-c\ell) \sum_{T\in\mathcal{T}_H} \|D(\mathcal{Q}_T^\ell y_H)\|_{L^2(\mathsf{N}^\ell(T))}\|De\|_{L^2(R_T)},
\end{aligned}
$$

where we have applied Theorem 4.1 to (5.12), treating $\mathsf{N}^\ell(T)$ as the whole domain.

The result then follows as in Theorem 5.1, using a discrete Cauchy–Schwarz inequality and the stability of $\mathcal{Q}_T^\ell$. The latter holds since

$$
\begin{aligned}
\alpha\|D(\mathcal{Q}_T^\ell y_H)\|^2_{L^2(\mathsf{N}^\ell(T))} &\le \mathfrak{a}(\mathcal{Q}_T^\ell y_H, \mathcal{Q}_T^\ell y_H) \\
&= (y_H, A : D(\mathcal{Q}_T^\ell y_H) + b\cdot(\mathcal{Q}_T^\ell y_H))_{L^2(T)} \\
&\le \|y_H\|_{L^2(T)}(\|A\|_{L^\infty} + C_{\mathrm{P}}^{-1}\|b\|_{L^\infty})\|D(\mathcal{Q}_T^\ell y_H)\|_{L^2(\mathsf{N}^\ell(T))},
\end{aligned}
$$

which concludes the proof. □

6. Practical multiscale method

In this section, we introduce a practical multiscale method based on locally computed basis functions. This is justified by the exponential decay of the globally defined prototypical basis functions and the localization results in Theorem 5.1 and Theorem 5.2. For each $F\in\mathcal{F}_H$, we define the localized basis function

$$
\tilde{\varphi}_F^\ell \coloneqq \mathcal{R}^\ell\rho_F. \tag{6.1}
$$

We define the localized multiscale space as their span, i.e.,

$$
\tilde{V}_H^\ell \coloneqq \operatorname{span}\{\tilde{\varphi}_F^\ell \,:\, F\in\mathcal{F}_H\}.
$$

We emphasize that the operator $\mathcal{R}^\ell$ depends on its argument only through the quantities of interest, as introduced in (3.1). Consequently, the definition (6.1) of $\tilde{\varphi}_F^\ell$ is independent of the specific choice of bubble functions, provided the Kronecker-delta condition (3.13) on the quantities of interest is satisfied.

The localized multiscale method now seeks the unique function $\tilde{z}_H\in\tilde{V}_H^\ell$ such that

$$
\forall\tilde{v}_H^\ell\in\tilde{V}_H^\ell: \quad \mathfrak{a}(\tilde{z}_H^\ell, \tilde{v}_H^\ell) = (f, A : D\tilde{v}_H^\ell + b\cdot\tilde{v}_H^\ell)_{L^2}. \tag{6.2}
$$

As a post-processing step, we then define

$$
\hat{z}_H^\ell \coloneqq \tilde{z}_H^\ell + \mathcal{Q}^\ell(\Pi_H f). \tag{6.3}
$$

The following theorem provides convergence results for the presented method.

Theorem 6.1 (Localized method)**.** *Let $z\in V$ be the solution to* (2.13) *and let $\hat{z}_H^\ell$ be the post-processed multiscale approximation defined in* (6.3)*. Then, we have the error bounds*

$$
\|D(z-\hat{z}_H^\ell)\|_{L^2} \lesssim H^{p+1}|f|_{H^{p+1}} + \ell^{(d-1)/2}\exp(-c\ell)\|f\|_{L^2}, \tag{6.4}
$$

$$
\|z-\hat{z}_H^\ell\|_{L^2} \lesssim H^{p+2}|f|_{H^{p+1}} + \ell^{(d-1)/2}\exp(-c\ell)\|f\|_{L^2}. \tag{6.5}
$$

Proof. Let $\hat{z}_H$ be the solution to (3.8) and $\tilde{z}_H\in\tilde{V}_H$ the solution to (3.5). By the triangle inequality, we have

$$
\|D(z-\hat{z}_H^\ell)\|_{L^2} \le \|D(z-\hat{z}_H)\|_{L^2} + \|D(\mathcal{Q}(\Pi_H f) - \mathcal{Q}^\ell(\Pi_H f))\|_{L^2} + \|D(\tilde{z}_H - \tilde{z}_H^\ell)\|_{L^2}. \tag{6.6}
$$

The first two terms can be bounded with Theorem 3.2 and Theorem 5.2, respectively. For the third term, we observe with $\tilde{z}_H = \mathcal{R}\tilde{z}_H$ that

$$\|D(\tilde{z}_H - \tilde{z}_H^\ell)\|_{L^2} \leq \|D(\mathcal{R}\tilde{z}_H - \mathcal{R}^\ell \tilde{z}_H)\|_{L^2} + \|D(\mathcal{R}^\ell \tilde{z}_H - \tilde{z}_H^\ell)\|_{L^2}. \tag{6.7}$$

The first term can be estimated with Theorem 5.1. For the second term in (6.7), using that $v = \mathcal{R}^\ell v$ for $v \in \tilde{V}_H^\ell$ and writing $\tilde{L}\varphi \coloneqq A : D\varphi + b \cdot \varphi$ for $\varphi \in V$, we obtain

$$\begin{aligned}
&\|D(\mathcal{R}^\ell \tilde{z}_H - \tilde{z}_H^\ell)\|_{L^2} \\
&\quad\lesssim \sup_{v \in \tilde{V}_H^\ell \setminus \{0\}} \frac{\mathfrak{a}(\mathcal{R}^\ell \tilde{z}_H - \tilde{z}_H^\ell, v)}{\|Dv\|_{L^2}} \\
&\quad= \sup_{v \in \tilde{V}_H^\ell \setminus \{0\}} \frac{\mathfrak{a}(\mathcal{R}^\ell \tilde{z}_H - \mathcal{R}\tilde{z}_H + \tilde{z}_H - \tilde{z}_H^\ell, v)}{\|Dv\|_{L^2}} \\
&\quad\lesssim \|D(\mathcal{R}\tilde{z}_H - \mathcal{R}^\ell \tilde{z}_H)\|_{L^2} + \sup_{v \in \tilde{V}_H^\ell \setminus \{0\}} \frac{\mathfrak{a}(\tilde{z}_H, v) - (f, \tilde{L}v)_{L^2}}{\|Dv\|_{L^2}} \\
&\quad= \|D(\mathcal{R}\tilde{z}_H - \mathcal{R}^\ell \tilde{z}_H)\|_{L^2} + \sup_{v \in \tilde{V}_H^\ell \setminus \{0\}} \frac{\mathfrak{a}(\tilde{z}_H, \mathcal{R}^\ell v - \mathcal{R}v) - (f, \tilde{L}(\mathcal{R}^\ell v - \mathcal{R}v))_{L^2}}{\|Dv\|_{L^2}} \\
&\quad\lesssim \ell^{(d-1)/2} \exp(-c\ell)\|f\|_{L^2},
\end{aligned}$$

where we have used Theorem 5.1 and the stability of $\tilde{z}_H$ in the final step.

Now, we combine this with (6.7) and once again Theorem 5.1, which yields

$$\|D(\tilde{z}_H - \tilde{z}_H^\ell)\|_{L^2} \lesssim \ell^{(d-1)/2} \exp(-c\ell)\|f\|_{L^2}. \tag{6.8}$$

Finally, we plug this into (6.6) and use Theorem 3.2 and Theorem 5.2 to obtain

$$\|D(z - \hat{z}_H^\ell)\|_{L^2} \lesssim H^{p+1}|f|_{H^{p+1}} + \ell^{(d-1)/2} \exp(-c\ell)\|f\|_{L^2},$$

which is the claimed bound (6.4).

To show the L^2-estimate, we define $r \in V$ as the auxiliary solution to

$$\forall v \in V\colon \quad \mathfrak{a}(r, v) = (z - \hat{z}_H^\ell, v)_{L^2}. \tag{6.9}$$

Further, $\tilde{r}_H \in \tilde{V}_H$ is the corresponding ideal multiscale approximation that solves

$$\forall \tilde{v}_H \in \tilde{V}_H\colon \quad \mathfrak{a}(\tilde{r}_H, \tilde{v}_H) = (z - \hat{z}_H^\ell, \tilde{v}_H)_{L^2}.$$

Note that $r - \tilde{r}_H \in W$ by the Galerkin orthogonality. Therefore, we have with Lemma 3.1 that

$$\|D(r - \tilde{r}_H)\|_{L^2}^2 \lesssim \mathfrak{a}(r - \tilde{r}_H, r - \tilde{r}_H) = (z - \hat{z}_H^\ell, r - \tilde{r}_H)_{L^2} \lesssim H\|z - \hat{z}_H^\ell\|_{L^2}\|D(r - \tilde{r}_H)\|_{L^2}$$

and thus,

$$\|D(r - \tilde{r}_H)\|_{L^2} \lesssim H\|z - \hat{z}_H^\ell\|_{L^2}. \tag{6.10}$$

Using $v = z - \hat{z}_H^\ell$ as a test function in (6.9), we obtain with (6.10), Theorem 3.2, and Theorem 5.2 that

$$\begin{aligned}
\|z - \hat{z}_H^\ell\|_{L^2}^2 &= \mathfrak{a}(r, z - \hat{z}_H^\ell) \\
&= \mathfrak{a}(r, z - \hat{z}_H) + \mathfrak{a}(r, \mathcal{Q}(\Pi_H f) - \mathcal{Q}^\ell(\Pi_H f)) + \mathfrak{a}(r, \tilde{z}_H - \tilde{z}_H^\ell) \\
&= \mathfrak{a}(r - \tilde{r}_H, z - \hat{z}_H) + \mathfrak{a}(r - \tilde{r}_H, \mathcal{Q}(\Pi_H f) - \mathcal{Q}^\ell(\Pi_H f)) + \mathfrak{a}(r, \tilde{z}_H - \tilde{z}_H^\ell) \\
&\lesssim H\|z - \hat{z}_H^\ell\|_{L^2}\big(\|D(z - \hat{z}_H)\|_{L^2} + \ell^{(d-1)/2} \exp(-c\ell)\|f\|_{L^2}\big) \\
&\qquad + \|z - \hat{z}_H^\ell\|_{L^2}\|\tilde{z}_H - \tilde{z}_H^\ell\|_{L^2}.
\end{aligned}$$

Using the Poincaré-type inequality (2.5) and employing (6.8), we finally get

$$\|z - \hat{z}_H^\ell\|_{L^2}^2 \lesssim \|z - \hat{z}_H^\ell\|_{L^2}\big(H\|D(z - \hat{z}_H)\|_{L^2} + H\ell^{(d-1)/2} \exp(-c\ell)\|f\|_{L^2}$$

$$+ \ell^{(d-1)/2}\exp(-c\ell)\|f\|_{L^2}\big).$$

In view of (3.9), we obtain the claimed bound (6.5). □

The practical multiscale method analyzed in Theorem 6.1 produces an approximation $\hat{z}_H^\ell$ to $z = \nabla u$ in the H^1-norm, where we recall that $u \in H^2(\Omega)\cap H_0^1(\Omega)$ is the unique strong solution to (2.1). Let us conclude this section with a brief discussion on the recovery of an approximation to u in the L^2-norm.

In the spirit of Lemma 2.5, let $\hat{u} \in H^2(\Omega)\cap H_0^1(\Omega)$ denote the unique solution to the problem

$$\begin{cases} \Delta\hat{u} = \nabla\cdot\hat{z}_H^\ell & \text{in } \Omega,\\ \hat{u} = 0 & \text{on } \partial\Omega, \end{cases} \tag{6.11}$$

and let $\hat{u}_{\mathcal{H}}$ denote an $H_0^1(\Omega)$-conforming $\mathcal{P}^1$-finite element approximation to $\hat{u}$ on a (coarse) mesh $\mathcal{T}_{\mathcal{H}}$. Here, $\mathcal{T}_{\mathcal{H}}$ is an element of a quasi-uniform and shape-regular family $\{\mathcal{T}_{\mathcal{H}}\}_{\mathcal{H}>0}$ of geometrically conformal meshes of Ω, where $\mathcal{H}\in(0,H]$ denotes the maximum diameter of elements in $\mathcal{T}_{\mathcal{H}}$. Note that $\mathcal{T}_{\mathcal{H}} = \mathcal{T}_H$ is an admissible choice. In view of Theorem 2.3, Lemma 2.5, and (6.11), we have that $\|u-\hat{u}\|_{H^1}\lesssim \|z-\hat{z}_H^\ell\|_{L^2}$ and

$$\|\hat{u}-\hat{u}_{\mathcal{H}}\|_{L^2} + \mathcal{H}\,|\hat{u}-\hat{u}_{\mathcal{H}}|_{H^1} \lesssim \mathcal{H}^2\|\nabla\cdot\hat{z}_H^\ell\|_{L^2} \lesssim \mathcal{H}^2\|D(z-\hat{z}_H^\ell)\|_{L^2} + \mathcal{H}^2\|f\|_{L^2}.$$

Hence, by the triangle inequality and Theorem 6.1, we obtain the L^2-error bound

$$\|u-\hat{u}_{\mathcal{H}}\|_{L^2} \lesssim H^{p+2}|f|_{H^{p+1}} + \Big(\ell^{(d-1)/2}\exp(-c\ell) + \mathcal{H}^2\Big)\,\|f\|_{L^2}.$$

In particular, if $\mathcal{T}_{\mathcal{H}}$ is constructed such that $\mathcal{H}\lesssim H^{1+\frac{p}{2}}$, then

$$\|u-\hat{u}_{\mathcal{H}}\|_{L^2} \lesssim H^{p+2}\|f\|_{H^{p+1}} + \ell^{(d-1)/2}\exp(-c\ell)\|f\|_{L^2}.$$

7. Implementation and numerical experiments

In this section, we discuss the implementation of the proposed multiscale method and present numerical experiments supporting the theoretical results of this paper. Note that all numerical experiments can be reproduced using the code available at `https://github.com/moimmahauck/NonDiv_LOD`.

7.1. Choice of quasi-interpolation $\mathcal{I}_H$.

For the definition of the operator $\mathcal{K}$ in (5.1), we require a quasi-interpolation operator $\mathcal{I}_H : V \to V_H$ satisfying the approximation and stability properties stated in (5.2). In the two-dimensional case, a possible choice of $\mathcal{I}_H$ is obtained by prescribing its nodal values at each interior node z via

$$(\mathcal{I}_H v)(z) \coloneqq \begin{bmatrix} n_{F_1}^1 & n_{F_1}^2 \\ n_{F_2}^1 & n_{F_2}^2 \end{bmatrix}^{-1} \begin{bmatrix} |F_1|^{-1}\int_{F_1} v\cdot n_{F_1}\,\mathrm{d}s \\ |F_2|^{-1}\int_{F_2} v\cdot n_{F_2}\,\mathrm{d}s \end{bmatrix}, \tag{7.1}$$

where F_1 and F_2 are two faces adjacent to z such that their corresponding unit normal vectors $n_{F_1} = (n_{F_1}^1, n_{F_1}^2)$ and $n_{F_2} = (n_{F_2}^1, n_{F_2}^2)$ are linearly independent. For boundary nodes, an analogous construction is applied, yielding a discrete function v_H that does not, in general, satisfy the tangential boundary conditions of the space V. Conformity with respect to the space V is then enforced by a suitable post-processing step: namely, the nodal values of v_H at the boundary are modified so as to eliminate its tangential component $v_H - (v_H\cdot n)n$. In the simple case of a square domain, this procedure reduces to setting one component of the nodal boundary values of v_H to zero. Construction (7.1), together with the post-processing step to enforce conformity with the space V, extends naturally to three dimensions by selecting, for each interior node z, three adjacent faces whose normal vectors are

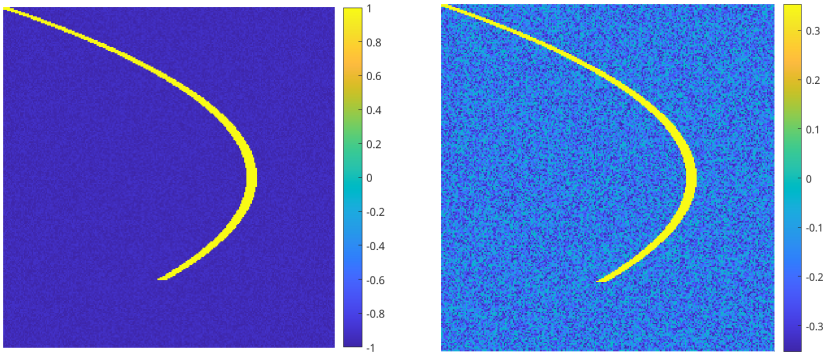

FIGURE 7.1. Illustration of the multiscale coefficients a_{12} (left) and b_1 (right) used in the numerical experiment.

linearly independent. The stability and approximation properties stated in (5.2) can be verified by following the arguments in [EG04, Ch. 1.6].

7.2. **Fine-scale discretization.** To compute the basis functions of the proposed multiscale method, the problems (5.6) and (5.12), associated with the operators $\mathcal{K}_T^\ell$ and $\mathcal{Q}_T^\ell$, respectively, must be solved. Although these problems are local, they remain infinite-dimensional and therefore require a fine-scale discretization. To this end, we introduce a fine mesh $\mathcal{T}_h$ obtained by refining the coarse mesh $\mathcal{T}_H$. The fine mesh must be sufficiently fine to resolve all microscopic features of the coefficients. The problems (5.6) and (5.12) are then solved on local $\mathcal{P}^1$-finite element spaces defined on submeshes of $\mathcal{T}_h$. In the fully discrete convergence analysis, the continuous space V is replaced by the fine-scale finite element space, and most arguments carry over directly; see, e.g., [MP20, Ch. 4.4]. This yields an a priori error estimate for the fully discrete LOD approximation with respect to the fine-scale finite element solution, analogous to Theorem 6.1. An estimate with respect to the solution of the original PDE then follows by applying the triangle inequality together with standard finite element approximation results.

7.3. **Numerical experiments.** For the numerical experiments, we consider the domain $\Omega := (0,1)^2$ and choose the stabilization parameter $\sigma := 1$ in (2.12). In this setting, the Poincaré constant (2.5) for the space V is given by $C_\mathrm{P} = \pi$. Therefore, the admissible range of δ in the Cordes-type condition (2.3) is $\delta \in (\frac{1}{1+\pi^2}, 1]$.

We choose the data of the numerical experiment as

$$A(x,y) := \begin{pmatrix} \frac{\sqrt{11}}{4} & a_{12}(x,y) \\ a_{12}(x,y) & \frac{3\sqrt{11}}{4} \end{pmatrix}, \quad b(x,y) := \begin{pmatrix} b_1(x,y) \\ 1 \end{pmatrix}, \quad f(x,y) := \cos(\pi x) y^3$$

for $(x,y) \in \Omega$, where a_{12} is a realization of a background random field that is piecewise constant on a Cartesian mesh with mesh size $\epsilon = 2^{-8}$, with independent and identically distributed values in the interval $[-1,-0.9]$, augmented by a channel taking the constant value 1. This channel consists of the elements whose midpoints have a distance less than 4ϵ from a parabola, the corresponding element values are set to 1. Analogously, we define b_1, with realizations in the interval $[-1/\sqrt{8}, 0]$, augmented by a channel taking the value $1/\sqrt{8}$. For an illustration of the multiscale coefficients a_{12} and b_1, we refer to Figure 7.1. It is quickly checked that the pair (A,b) satisfies the Cordes-type condition (2.3) with $\delta = \frac{1}{10} \in \big(\frac{1}{1+\pi^2}, 1\big]$.

For the multiscale approximation, we construct a hierarchy of meshes by uniformly refining the initial mesh shown in Figure 7.2 (left). For simplicity, we denote the meshes in this hierarchy by $\mathcal{T}_{2^0}, \mathcal{T}_{2^{-1}}, \dots, \mathcal{T}_{2^{-6}}$, where the subscript indicates the

side length of the squares formed by joining opposing triangles. For the fine-scale discretization, we use the mesh $\mathcal{T}_{2^{-9}}$, and the corresponding fine-scale approximation is denoted by z_h. In the following, we study the approximation errors of the fine-scale discretized counterparts of the original and post-processed multiscale approximations defined in (6.2) and (6.3), denoted by $\tilde{z}^\ell_{H,h}$ and $\hat{z}^\ell_{H,h}$, respectively. Specifically, we consider the energy errors

$$\operatorname{err}_{\mathfrak{a}}(H,\ell) \coloneqq \|z_h - \tilde{z}^\ell_{H,h}\|_{\mathfrak{a}}, \qquad \operatorname{err}^{\mathrm{pp}}_{\mathfrak{a}}(H,\ell) \coloneqq \|z_h - \hat{z}^\ell_{H,h}\|_{\mathfrak{a}},$$

where $\|\cdot\|_{\mathfrak{a}}$ denotes the energy norm induced by the bilinear form $\mathfrak{a}$. We recall that, in view of Lemma 2.4, the energy norm is equivalent to the norm $\|D(\cdot)\|_{L^2}$.

For the multiscale approximation without post-processing, as defined in (6.2), Figure 7.2 shows that the error decreases with mesh refinement, but the convergence is very slow, with estimated convergence rates well below one. This behavior is due to the low regularity of the right-hand side of the variational problem (2.13), which lies only in the dual space V^*. Consequently, no rigorous convergence rates can be extracted; see Remark 3.3.

However, post-processing as introduced in (6.3) changes the picture completely. This post-processing allows one to extract convergence rates from the right-hand side despite the low regularity of the corresponding functional. This is clearly visible in Figure 7.3, where, for sufficiently large oversampling parameters, second- and third-order convergence is observed for the post-processed approximations with $p = 1$ and $p = 2$, respectively. For the post-processing, we choose the operator Π_H in (3.6) as the nodal interpolation onto first-order ($p = 1$) and second-order ($p = 2$) Lagrange finite element spaces defined on the mesh $\mathcal{T}_H$. These numerical observations are in line with the theoretical predictions from Theorem 6.1. Note that, for fixed oversampling parameters ℓ, the errors initially decrease with optimal order but eventually reach a plateau, the value of which depends on the specific choice of ℓ. This behavior is consistent with the theoretical prediction in Theorem 6.1 and contrasts with the results in [FGPS24], where, for fixed oversampling parameters, the error initially decreases but then increases sharply. The increase is caused by a negative power of H multiplying the (exponentially decaying) localization error in the error estimate. Here, this issue is avoided by adapting the localization strategy proposed in [HLM26].

We emphasize that, by employing this new post-processing, convergence can be shown in an H^2-type norm of the solution u which was not possible in previous work; see [FGPS24].

Acknowledgments. The authors are grateful to D. Gallistl (Friedrich-Schiller-Universität Jena) for providing a monoscale code that served as the foundation for the implementation developed in this work. M. Hauck and R. Maier acknowledge funding from the Deutsche Forschungsgemeinschaft (DFG, German Research Foundation) – Project-ID 258734477 – SFB 1173. Parts of this work were conducted during M. Hauck's and R. Maier's stay at the Hausdorff Research Institute for Mathematics funded by the Deutsche Forschungsgemeinschaft (DFG, German Research Foundation) under Germany's Excellence Strategy – EXC-2047/2 – 390685813.

References

[AFL22] S. Armstrong, B. Fehrman, and J. Lin. Green function and invariant measure estimates for nondivergence form elliptic homogenization, 2022. arXiv:2211.13279.

[AHP21] R. Altmann, P. Henning, and D. Peterseim. Numerical homogenization beyond scale separation. *Acta Numerica*, 30:1–86, 2021.

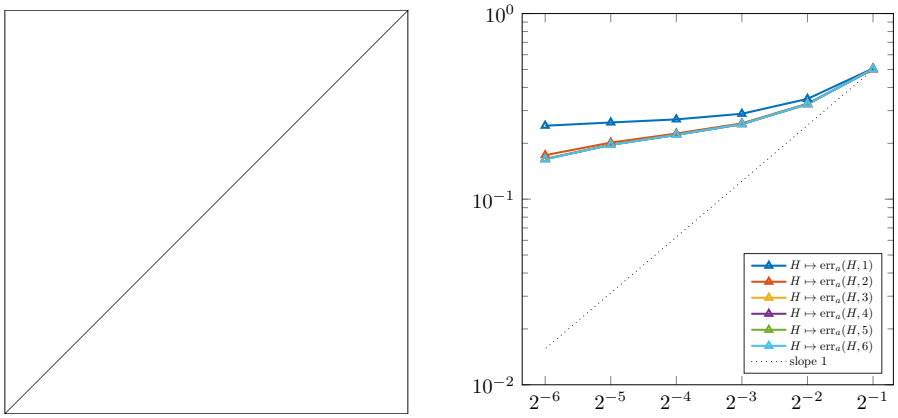

FIGURE 7.2. Initial mesh for the mesh generation (left). Energy errors of the multiscale approximation $\tilde{z}_{H,h}^{\ell}$ (without post-processing) for different choices of the oversampling parameter ℓ, plotted as a function of the coarse mesh size H (right).

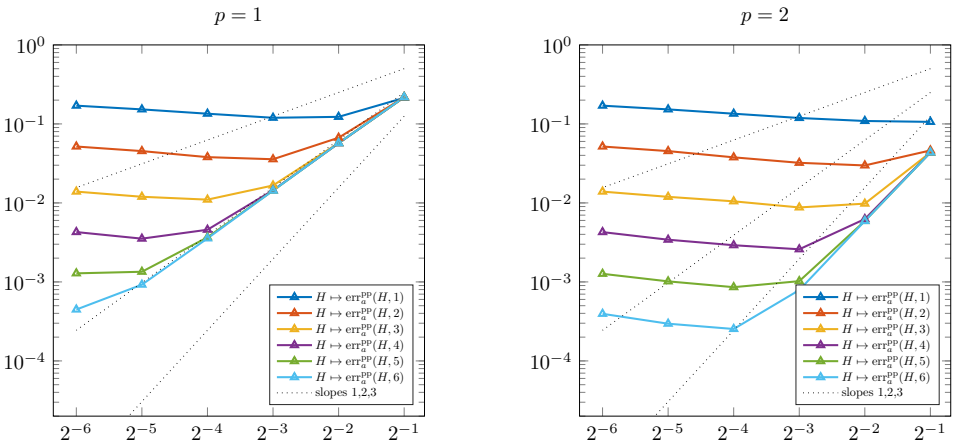

FIGURE 7.3. Energy errors of the post-processed multiscale approximation $\hat{z}_{H,h}^{\ell}$ for different choices of the oversampling parameter ℓ, plotted as a function of the coarse mesh size H. Two choices for the polynomial degree used for the post-processing (cf. (3.8) and (6.3)) are considered: $p = 1$ (left) and $p = 2$ (right).

[BBF13] D. Boffi, F. Brezzi, and M. Fortin. *Mixed finite element methods and applications*. Springer, Heidelberg, 2013.

[Bis88] N. T. Bishop. The Poincaré inequality for a vector field with zero tangential or normal component on the boundary. *Quaestiones Math.*, 11(2):195–199, 1988.

[Cam94] S. Campanato. On the condition of nearness between operators. *Ann. Mat. Pura Appl. (4)*, 167:243–256, 1994.

[CM09] F. Camilli and C. Marchi. Rates of convergence in periodic homogenization of fully nonlinear uniformly elliptic PDEs. *Nonlinearity*, 22(6):1481–1498, 2009.

[Cor56] H. O. Cordes. Über die erste Randwertaufgabe bei quasilinearen Differentialgleichungen zweiter Ordnung in mehr als zwei Variablen. *Math.*

Ann., 131:278–312, 1956.

[CSS20] Y. Capdeboscq, T. Sprekeler, and E. Süli. Finite element approximation of elliptic homogenization problems in nondivergence-form. *ESAIM Math. Model. Numer. Anal.*, 54(4):1221–1257, 2020.

[DHM23] Z. Dong, M. Hauck, and R. Maier. An improved high-order method for elliptic multiscale problems. *SIAM J. Numer. Anal.*, 61(4):1918–1937, 2023.

[DPE11] D.A. Di Pietro and A. Ern. *Mathematical Aspects of Discontinuous Galerkin Methods*. Mathématiques et Applications. Springer Berlin Heidelberg, 2011.

[EG04] A. Ern and J.-L. Guermond. *Theory and Practice of Finite Elements*, volume 159 of *Applied Mathematical Sciences*. Springer New York, 2004.

[FGPS24] P. Freese, D. Gallistl, D. Peterseim, and T. Sprekeler. Computational multiscale methods for nondivergence-form elliptic partial differential equations. *Comput. Methods Appl. Math.*, 24(3):649–672, 2024.

[FO09] B. D. Froese and A. M. Oberman. Numerical averaging of nondivergence structure elliptic operators. *Commun. Math. Sci.*, 7(4):785–804, 2009.

[FO18a] C. Finlay and A. M. Oberman. Approximate homogenization of convex nonlinear elliptic PDEs. *Commun. Math. Sci.*, 16(7):1895–1906, 2018.

[FO18b] C. Finlay and A. M. Oberman. Approximate homogenization of fully nonlinear elliptic PDEs: estimates and numerical results for Pucci type equations. *J. Sci. Comput.*, 77(2):936–949, 2018.

[Gal17] D. Gallistl. Variational formulation and numerical analysis of linear elliptic equations in nondivergence form with Cordes coefficients. *SIAM J. Numer. Anal.*, 55(2):737–757, 2017.

[Gal19] D. Gallistl. Numerical approximation of planar oblique derivative problems in nondivergence form. *Math. Comp.*, 88(317):1091–1119, 2019.

[GSS21] D. Gallistl, T. Sprekeler, and E. Süli. Mixed Finite Element Approximation of Periodic Hamilton–Jacobi–Bellman Problems With Application to Numerical Homogenization. *Multiscale Model. Simul.*, 19(2):1041–1065, 2021.

[GST25a] X. Guo, T. Sprekeler, and H. V. Tran. Characterizations of diffusion matrices in homogenization of elliptic equations in nondivergence-form. *Calc. Var. Partial Differential Equations*, 64(1), 2025. Paper No. 1.

[GST25b] X. Guo, T. Sprekeler, and H. V. Tran. Homogenization of nondivergence form operators in i.i.d. random environments, 2025. arXiv:2512.04410.

[GT24] X. Guo and H. V. Tran. Stochastic integrability of heat-kernel bounds for random walks in a balanced random environment. *Electron. J. Probab.*, 29, 2024. Paper No. 194.

[GT25] X. Guo and H. V. Tran. Optimal convergence rates in stochastic homogenization in a balanced random environment. *Probab. Theory Related Fields*, 193(3-4):821–880, 2025.

[GTY20] X. Guo, H. V. Tran, and Y. Yu. Remarks on optimal rates of convergence in periodic homogenization of linear elliptic equations in nondivergence form. *Partial Differ. Equ. Appl.*, 1(4), 2020. Paper No. 15.

[HHM16] F. Hellman, P. Henning, and A. Målqvist. Multiscale mixed finite elements. *Discrete Contin. Dyn. Syst. Ser. S*, 9(5):1269–1298, 2016.

[HL25a] M. Hauck and A. Lozinski. A high-order localized orthogonal decomposition method for heterogeneous Stokes problems, 2025. arXiv:2511.22684.

[HL25b] M. Hauck and A. Lozinski. A localized orthogonal decomposition method for heterogeneous Stokes problems. *SIAM J. Numer. Anal.*, 63(4):1617–1641, 2025.

[HLM26] M. Hauck, A. Lozinski, and R. Maier. A generalized framework for higher-order localized orthogonal decomposition methods. *ESAIM Math. Model. Numer. Anal.*, 60(1):445–471, 2026.

[HLS26] P. Henning, H. Li, and T. Sprekeler. Stable localized orthogonal decomposition in Raviart-Thomas spaces. *IMA J. Numer. Anal.*, in press, 2026.

[HM17] F. Hellman and A. Målqvist. Contrast independent localization of multiscale problems. *Multiscale Model. Simul.*, 15:1325–1355, 2017.

[HM19] F. Hellman and A. Målqvist. Numerical homogenization of elliptic PDEs with similar coefficients. *Multiscale Model. Simul.*, 17(2):650–674, 2019.

[HMM25] M. Hauck, A. Målqvist, and M. Mosquera. A localized orthogonal decomposition method for heterogeneous mixed-dimensional problems, 2025. arXiv:2510.09442.

[HP22a] M. Hauck and D. Peterseim. Multi-resolution localized orthogonal decomposition for helmholtz problems. *Multiscale Model. Sim.*, 20(2):657–684, 2022.

[HP22b] M. Hauck and D. Peterseim. Super-localization of elliptic multiscale problems. *Math. Comp.*, 92(341):981–1003, 2022.

[KKMW25] B. Kalyanaraman, F. Krumbiegel, R. Maier, and S. Wang. Optimal higher-order convergence rates for parabolic multiscale problems, 2025. arXiv:2510.09514.

[KM19] R. C. Kirby and L. Mitchell. Code generation for generally mapped finite elements. *ACM Trans. Math. Software*, 45(4):Art. 41, 23, 2019.

[KS22] E. L. Kawecki and T. Sprekeler. Discontinuous Galerkin and C^0-IP finite element approximation of periodic Hamilton-Jacobi-Bellman-Isaacs problems with application to numerical homogenization. *ESAIM Math. Model. Numer. Anal.*, 56(2):679–704, 2022.

[Mai21] R. Maier. A high-order approach to elliptic multiscale problems with general unstructured coefficients. *SIAM J. Numer. Anal.*, 59(2):1067–1089, 2021.

[MP14] A. Målqvist and D. Peterseim. Localization of elliptic multiscale problems. *Math. Comp.*, 83(290):2583–2603, 2014.

[MP20] A. Målqvist and D. Peterseim. *Numerical Homogenization by Localized Orthogonal Decomposition*. Society for Industrial and Applied Mathematics, 2020.

[QSTY24] J. Qian, T. Sprekeler, H. V. Tran, and Y. Yu. Optimal Rate of Convergence in Periodic Homogenization of Viscous Hamilton-Jacobi Equations. *Multiscale Model. Simul.*, 22(4):1558–1584, 2024.

[Spr24] T. Sprekeler. Homogenization of nondivergence-form elliptic equations with discontinuous coefficients and finite element approximation of the homogenized problem. *SIAM J. Numer. Anal.*, 62(2):646–666, 2024.

[Spr26] T. Sprekeler. A Cordes framework for stationary Fokker–Planck–Kolmogorov equations, 2026. arXiv:2601.14548.

[SS13] I. Smears and E. Süli. Discontinuous Galerkin finite element approximation of nondivergence form elliptic equations with Cordès coefficients. *SIAM J. Numer. Anal.*, 51(4):2088–2106, 2013.

[SS14] I. Smears and E. Süli. Discontinuous Galerkin finite element approximation of Hamilton-Jacobi-Bellman equations with Cordes coefficients. *SIAM J. Numer. Anal.*, 52(2):993–1016, 2014.

[SSZ25] T. Sprekeler, E. Süli, and Z. Zhang. Finite element approximation of stationary Fokker-Planck-Kolmogorov equations with application to periodic numerical homogenization. *SIAM J. Numer. Anal.*, 63(3):1315–1343, 2025.

[ST21] T. Sprekeler and H. V. Tran. Optimal convergence rates for elliptic homogenization problems in nondivergence-form: analysis and numerical illustrations. *Multiscale Model. Simul.*, 19(3):1453–1473, 2021.

[SWZ25] T. Sprekeler, H. Wu, and Z. Zhang. Numerical approximation of effective diffusivities in homogenization of nondivergence-form equations with large drift by a Lagrangian method, 2025. arXiv:2506.14073.

[Tal65] G. Talenti. Sopra una classe di equazioni ellittiche a coefficienti misurabili. *Ann. Mat. Pura Appl. (4)*, 69:285–304, 1965.

* Institute for Applied and Numerical Mathematics, Karlsruhe Institute of Technology, Englerstr. 2, 76131 Karlsruhe, Germany

Email address: {moritz.hauck,roland.maier}@kit.edu

† Department of Mathematics, Texas A&M University, College Station, TX 77843, USA

Email address: timo.sprekeler@tamu.edu